

NAVAL POSTGRADUATE SCHOOL Monterey, California



THESIS

ANALYSIS OF M-JPEG VIDEO OVER AN ATM NETWORK

by

Albert C. Kinney

June 2001

Thesis Advisor:
Second Reader:

John McEachen
Murali Tummala

Approved for public release; distribution is unlimited.

Form SF298 Citation Data

Report Date <i>("DD MON YYYY")</i> 15 Jun 2001	Report Type N/A	Dates Covered (from... to) <i>("DD MON YYYY")</i>
Title and Subtitle ANALYSIS OF M-JPEG VIDEO OVER AN ATM NETWORK		Contract or Grant Number
		Program Element Number
Authors		Project Number
		Task Number
		Work Unit Number
Performing Organization Name(s) and Address(es) Naval Postgraduate School Monterey, CA 93943-5138		Performing Organization Number(s)
Sponsoring/Monitoring Agency Name(s) and Address(es)		Monitoring Agency Acronym
		Monitoring Agency Report Number(s)
Distribution/Availability Statement Approved for public release, distribution unlimited		
Supplementary Notes		
Abstract		
Subject Terms		
Document Classification unclassified	Classification of SF298 unclassified	
Classification of Abstract unclassified	Limitation of Abstract unlimited	
Number of Pages 105		

ANALYSIS OF M-JPEG VIDEO OVER AN ATM NETWORK

Albert C. Kinney-Lieutenant Commander, United States Navy

B.S., U.S. Naval Academy, 1989

Master of Science in Electrical Engineering-June 2001

Advisor: John McEachen, Department of Electrical Engineering

Second Reader: Murali Tummala, Department of Electrical Engineering

With the emergence of a network-centric philosophy of military operations, the behavior of video applications over resource-constrained information networks is of increasing interest in the development of future naval information systems. This thesis analyzes the impact of compression, delay variance, and channel noise on perceived networked video quality using commercially available off-the-shelf equipment and software. An experimental setup for packet video is developed for quantitative and qualitative analysis of Motion JPEG video transmitted over a constrained Asynchronous Transfer Mode (ATM) network. Bandwidth profile analysis for various types of video points out the impracticality of ATM bandwidth and cell delay management algorithms for mainstream video applications, such as entertainment and distance learning. Additionally, functional limitations of individual system components are identified for consideration in the planning of future experimental work.

DoD KEY TECHNOLOGY AREA: Command, Control and Communications

KEYWORDS: ATM, PROTOCOL, MOTION JPEG, PACKET VIDEO, COMMUNICATIONS

REPORT DOCUMENTATION PAGE			<i>Form Approved OMB No. 0704-0188</i>
Public reporting burden for this collection of information is estimated to average 1 hour per response, including the time for reviewing instruction, searching existing data sources, gathering and maintaining the data needed, and completing and reviewing the collection of information. Send comments regarding this burden estimate or any other aspect of this collection of information, including suggestions for reducing this burden, to Washington headquarters Services, Directorate for Information Operations and Reports, 1215 Jefferson Davis Highway, Suite 1204, Arlington, VA 22202-4302, and to the Office of Management and Budget, Paperwork Reduction Project (0704-0188) Washington DC 20503.			
1. AGENCY USE ONLY (Leave blank)	2. REPORT DATE June 2001	3. REPORT TYPE AND DATES COVERED Master's Thesis	
4. TITLE AND SUBTITLE: Title (Mix case letters) Analysis of M-JPEG Video over an ATM Network		5. FUNDING NUMBERS	
6. AUTHOR(S) Albert C. Kinney		8. PERFORMING ORGANIZATION REPORT NUMBER	
7. PERFORMING ORGANIZATION NAME(S) AND ADDRESS(ES) Naval Postgraduate School Monterey, CA 93943-5000		10. SPONSORING / MONITORING AGENCY REPORT NUMBER	
9. SPONSORING / MONITORING AGENCY NAME(S) AND ADDRESS(ES) N/A		11. SUPPLEMENTARY NOTES The views expressed in this thesis are those of the author and do not reflect the official policy or position of the Department of Defense or the U.S. Government.	
12a. DISTRIBUTION / AVAILABILITY STATEMENT Approved for public release; distribution is unlimited.		12b. DISTRIBUTION CODE	
13. ABSTRACT (maximum 200 words) With the emergence of a network-centric philosophy of military operations, the behavior of video applications over resource-constrained information networks is of increasing interest in the development of future naval information systems. This thesis analyzes the impact of compression, delay variance, and channel noise on perceived networked video quality using commercially available off-the-shelf equipment and software. An experimental setup for packet video is developed for quantitative and qualitative analysis of Motion JPEG video transmitted over a constrained Asynchronous Transfer Mode (ATM) network. Bandwidth profile analysis for various types of video points out the impracticality of ATM bandwidth and cell delay management algorithms for mainstream video applications, such as entertainment and distance learning. Additionally, functional limitations of individual system components are identified for consideration in the planning of future experimental work.			
14. SUBJECT TERMS ATM, Protocol, Motion JPEG, Packet Video, Communications			15. NUMBER OF PAGES 107
			16. PRICE CODE
17. SECURITY CLASSIFICATION OF REPORT Unclassified	18. SECURITY CLASSIFICATION OF THIS PAGE Unclassified	19. SECURITY CLASSIFICATION OF ABSTRACT Unclassified	20. LIMITATION OF ABSTRACT UL

THIS PAGE INTENTIONALLY LEFT BLANK

Approved for public release; distribution is unlimited.

ANALYSIS OF M-JPEG VIDEO OVER AN ATM NETWORK

Albert C. Kinney
Lieutenant Commander, U.S. Navy
B.S., U.S. Naval Academy, 1989

Submitted in partial fulfillment of the
requirements for the degree of

MASTER OF SCIENCE IN ELECTRICAL ENGINEERING

from the

**NAVAL POSTGRADUATE SCHOOL
June 2001**

Author: _____
Albert C. Kinney

Approved by: _____
John C. McEachen, Thesis Advisor

Murali Tummala, Second Reader

Jeffrey B. Knorr, Chairman
Department of Electrical and Computer Engineering

THIS PAGE INTENTIONALLY LEFT BLANK

ABSTRACT

With the emergence of a network-centric philosophy of military operations, the behavior of video applications over resource-constrained information networks is of increasing interest in the development of future naval information systems. This thesis analyzes the impact of compression, delay variance, and channel noise on perceived networked video quality using commercially available off-the-shelf equipment and software. An experimental packet video laboratory is developed for quantitative and qualitative analysis of Motion JPEG video transmitted over a constrained Asynchronous Transfer Mode (ATM) network. Bandwidth profile analysis for various types of video points out the impracticality of ATM bandwidth and cell delay management algorithms for mainstream video applications such as entertainment and distance learning. Additionally, functional limitations of individual laboratory components are identified for consideration in the planning of future experimental work.

THIS PAGE INTENTIONALLY LEFT BLANK

TABLE OF CONTENTS

I.	INTRODUCTION.....	1
A.	BACKGROUND	1
B.	OBJECTIVES	3
C.	RELATED WORK.....	3
D.	THESIS ORGANIZATION.....	5
II.	ATM OVERVIEW.....	7
A.	INTRODUCTION.....	7
B.	ATM PROTOCOL REFERENCE MODEL.....	8
C.	ATM SWITCHING	10
D.	ATM TRAFFIC MANAGEMENT	11
1.	ATM Service Architecture	11
2.	ATM Quality of Service.....	13
3.	ATM Traffic Contract.....	15
4.	Traffic Contract Parameters and Related Algorithms.....	17
a.	<i>Cell Delay Variation Tolerance for PCR and SCR</i>	<i>17</i>
b.	<i>Generic Cell Rate Algorithm</i>	<i>17</i>
5.	CBR and VBR Traffic Contract Conformance Definitions.....	18
a.	<i>CBR.1: Conformance Definition for PCR (CLP=0+1)</i>	<i>18</i>
b.	<i>VBR.1: Conformance Definition for PCR (CLP=0+1) and SCR (CLP=0+1)</i>	<i>19</i>
c.	<i>VBR.2: Conformance Definition for PCR (CLP=0+1) and SCR (CLP=0)</i>	<i>19</i>
d.	<i>VBR.3: Conformance Definition for PCR (CLP=0+1) and SCR (CLP=0)</i>	<i>20</i>
6.	Usage Parameter Control.....	21
E.	SUMMARY	22
III.	MOTION JPEG COMPRESSION	23
A.	INTRODUCTION.....	23
B.	OVERVIEW OF THE SEQUENTIAL (BASELINE) JPEG COMPRESSION ALGORITHM.....	24
1.	Decomposition	25
2.	Discrete Cosine Transform	25
3.	Quantization – Scaling and Rounding	26
4.	Entropy Coding.....	26
C.	COMPRESSION AND PERFORMANCE.....	28
D.	SUMMARY	28
IV.	EQUIPMENT OVERVIEW	31
A.	AVA-300 VIDEO/AUDIO ENCODER.....	31
B.	ATV-300 VIDEO/AUDIO DECODER	32
C.	ASX-200BX ATM SWITCH.....	32
D.	SX/14 DATA CHANNEL SIMULATOR	33
E.	AX/4000 ATM TEST SYSTEM.....	34

1.	System Window	34
2.	Generator Module.....	35
3.	Analyzer Module.....	36
F.	SUMMARY	38
V.	DATA SETS, EXPERIMENTS, AND RESULTS	39
A.	VIDEO DATA SET CHARACTERISTICS.....	39
1.	Baseline TARZAN Video Clip	40
2.	Baseline TOYSTORY2 Video Clip	41
3.	Baseline WIZARD Video Clip	41
4.	Baseline DISTANCE Video Clip	42
5.	Bandwidth Profile Analysis.....	43
B.	ARCHITECTURE, ORGANIZATION, AND PROCEDURES.....	45
1.	Protocol Architecture	45
2.	Physical Network Description.....	46
3.	Data Collection Procedures.....	47
a.	<i>Effects of Intra-frame Compression on Video Performance</i>	47
b.	<i>Effects of Frame Rate on Video Performance</i>	48
c.	<i>Effects of Bandwidth-Managing UPC Contracts on Video Performance</i>	48
d.	<i>Effects of Delay Variation-Managing UPC Contracts on Video Performance</i>	49
e.	<i>Effects of Noise on Video Performance</i>	51
C.	RESULTS OF EXPERIMENTS	51
1.	Effect of Intra-frame Compression on Video Data Set Characteristics.....	51
2.	Effect of Frame Rate on Video Data Set Characteristics	59
3.	Effect of UPC on Video Data Set Characteristics	62
4.	Effect of Cell Delay Variation on M-JPEG Video Performance ...	67
5.	Effect of Noise on M-JPEG Video Performance	70
D.	SUMMARY	70
VI.	CONCLUSIONS AND RECOMMENDATIONS.....	73
A.	CONCLUSIONS REGARDING BANDWIDTH MANAGEMENT.....	73
B.	CONCLUSIONS REGARDING SECOND ORDER DELAY	74
C.	CONCLUSIONS REGARDING PERFORMANCE IN NOISE	75
D.	RECOMMENDATIONS FOR FUTURE WORK.....	75
	APPENDIX A: VIDEO TIMELINES	77
	APPENDIX B: DATA CHANNEL SIMULATOR PROGRAMMING FOR CDV.....	81
	LIST OF REFERENCES	83
	INITIAL DISTRIBUTION LIST	85

LIST OF FIGURES

Figure 2-1. ATM Protocol Reference Model from Ref. [1].	9
Figure 2-2. Virtual Channels within Virtual Paths from Ref. [1].	11
Figure 2-3. Dual Leaky Bucket GCRA from Ref. [6].	18
Figure 3-2. Zigzag Ordering of Coefficients from Ref. [11].	27
Figure 4-1. AX/4000 System Window.	35
Figure 4-2. AX/4000 Generator Dialog Box.	36
Figure 4-3. AX/4000 Analyzer Dialog Box.	37
Figure 4-4. Physical Network Configuration.	38
Figure 5-1. TARZAN Baseline Bandwidth Requirement.	40
Figure 5-2. TOYSTORY2 Baseline Bandwidth Requirement.	41
Figure 5-3. WIZARD Baseline Bandwidth Requirement.	42
Figure 5-4. DISTANCE Baseline Bandwidth Requirement.	43
Figure 5-5. Bandwidth Profiles for Baseline Data Sets.	45
Figure 5-6. Protocol Architecture.	46
Figure 5-7. Physical Network Configuration.	47
Figure 5-8. Statistics for TOYSTORY2 A.	50
Figure 5-9. Effect of Compression on TARZAN Video Clip.	52
Figure 5-10. Effect of Compression on TOYSTORY2 Video Clip.	53
Figure 5-11. Effect Compression on WIZARD Video Clip.	53
Figure 5-12. Effect of Compression on DISTANCE Video Clip.	54
Figure 5-13. Linear Effects of Compression on Video Data Sets.	55
Figure 5-14. Bandwidth Profiles for Compression Family E.	56
Figure 5-15. Cell Inter-arrival Time for TARZAN Compression Families.	57
Figure 5-16. Cell Inter-arrival Time for TOYSTORY2 Compression Families.	58
Figure 5-17. Cell Inter-arrival Time for WIZARD Compression Families.	58
Figure 5-18. Cell Inter-arrival Time for DISTANCE Compression Families.	59
Figure 5-19. Effect of Frame Rate on TARZAN Video Clip.	60
Figure 5-20. Effect of Frame Rate on TOYSTORY2 Video Clip.	60
Figure 5-21. Effect of Frame Rate on WIZARD Video Clip.	61
Figure 5-22. Effect of Frame Rate on DISTANCE Video Clip.	61
Figure 5-23. Effect of UPC 1 on TOYSTORY2.	62
Figure 5-24. Effect of UPC 2 on TOYSTORY2.	64
Figure 5-25. Effect of UPC 3 on TOYSTORY2.	64
Figure 5-26. Effect of UPC 4 on TOYSTORY2.	65
Figure 5-27. Effect of UPC 5 on TOYSTORY2.	65
Figure 5-28. Effect of CDVT on TOYSTORY2 Video Clip (CDVT = 300 μ Sec).	69
Figure 5-29. Effect of CDVT on TOYSTORY2 Video Clip (CDVT = 225 μ Sec).	69

THIS PAGE INTENTIONALLY LEFT BLANK

LIST OF TABLES

Table 4-1. AVA-300 User-Selectable Motion-JPEG Parameters	31
Table 5-1. Compression Families	39
Table 5-2. UPC Contracts	50

THIS PAGE INTENTIONALLY LEFT BLANK

LIST OF ABBREVIATIONS

AAL	ATM Adaptation Layer
ABR	Available Bit Rate
ASCII	American Standard Code for Information Interchange
ATM	Asynchronous Transfer Mode
BER	Bit Error Rate
BT	Burst Tolerance
CBR	Constant Bit Rate
CDV	Cell Delay Variation
CER	Cell Error Rate
CDVT	Cell Delay Variation Tolerance
CLP	Cell Loss Priority
CLR	Cell Loss Ratio
CMR	Cell Misinsertion Rate
cps	Cell Per Second
CTD	Cell Transfer Delay
DCT	Discrete Cosine Transform
DFT	Discrete Fourier Transform
DSP	Digital Signal Processing
fps	Frames Per Second
GCRA	Generic Cell Rate Algorithm
GFR	Guaranteed Frame Rate
HVS	Human Visual System
IDCT	Inverse Discrete Cosine Transform
IP	Internet Protocol
ISO	International Standards Organization
ITU	International Telecommunications Union
JPEG	Joint Photographic Experts Group
LAN	Local Area Network
LED	Light Emitting Diode
M-JPEG	Motion – Joint Photographic Experts Group
MBS	Maximum Burst Size
MCR	Minimum Cell Rate
Mbps	Megabits Per Second
MFS	Maximum Frame Size
NNI	Network to Network (Node to Node) Interface
NTSC	National Telecommunications Standards Committee
OAM	Operation, Administration, and Maintenance
OSI	Open Systems Interconnection
PAL	Phase Alternate Line
PCM	Pulse Coded Modulation
PCR	Peak Cell Rate
PDU	Protocol Data Unit
PMD	Physical Medium Dependent

PVC	Permanent Virtual Channel
QoS	Quality of Service
QT	Quantization Table
RLE	Run Length Encoding
RM	Resource Management
SC	Semi-Compressed
SAR	Segmentation and Reassembly
SCR	Sustainable Cell Rate
SECBR	Severely Errored Cell Block Ratio
SONET	Synchronous Optical Network
SVC	Switched Virtual Channel
TC	Transmission Convergence
TCP	Transport Control Protocol
UBR	Unspecified Bit Rate
UNI	User to Network Interface
UPC	Usage Parameter Control
VBR	Variable Bit Rate
VC	Virtual Circuit
VCC	Virtual Channel Connection
VCI	Virtual Channel Identifier
VP	Virtual Path
VPC	Virtual Path Connection
VPI	Virtual Path Identifier

EXECUTIVE SUMMARY

As the United States Navy moves toward a network-centric philosophy of operations, wide area network video applications will become critically important at the operational and tactical levels of warfare. Accelerated decision cycles and radical changes to traditional organizational structures will demand detailed intelligence products and immediate multi-node conferencing in support of modern warfare operations. Therefore, the behavior of information networks and video applications when constrained by various limitations is of increasing interest in the development of naval information systems. These limitations include network resource constraints, system configuration options, and extrinsic environmental conditions, such as distance and channel noise. This thesis explores some of these limitations and their effect on perceived video quality using commercially available off-the-shelf equipment and software.

High quality, live video is the most demanding network application due to its inherently high bandwidth and low delay requirements. Asynchronous Transfer Mode (ATM) addresses these requirements by providing high-throughput, bandwidth-managed links capable of delivering video data within the unique Quality of Service (QoS) constraints specified by individual users.

Video streams naturally generate very large amounts of data, which can easily exceed the available bandwidth in a network link. The Motion JPEG (M-JPEG) video compression scheme is popular in networked video applications due to its compression efficiency and the inherent error resilience properties of intra-frame encoding. In an intra-frame coded scheme, errors within a video frame do not propagate to subsequent frames. Additionally, M-JPEG video frames can be accessed arbitrarily throughout the sequence without regard to any inter-frame anchoring scheme.

Under its QoS rubric, the ATM Traffic Management Specification 4.1 provides several tools and algorithms to manage the limited bandwidth resource. Some of these QoS functions aim to distribute bandwidth efficiently while others seek to minimize

network congestion. In any case, a video stream that violates the agreed upon QoS contract will ultimately suffer cell loss.

Given the importance of networked video applications within the context of future naval information systems, this thesis analyzes the performance of a commercially available intra-frame coded video application under various network constraints. It seeks to understand the effects of the following variables on the perceived quality of the application: User-accessible M-JPEG encoding parameters, user-selectable ATM QoS parameters, simulated delay and delay variation, and noise.

As a concurrent objective of this work, a packet video experimentation module was developed within the Advanced Networking Laboratory. Functional limitations of the individual laboratory components are identified for consideration in planning future experimental work. This laboratory module will serve as a network application demonstrator and practical testing environment for various electrical engineering coursework and research activities.

This thesis concludes with several observations about the application and behavior of QoS mechanisms and network protocols within the given system architecture. Of note, experimental results point out the impracticality of ATM bandwidth and cell delay management algorithms for mainstream video applications, such as entertainment and distance learning. Additionally, network recovery time characteristics for various UPC-induced catastrophic synchronization failures are discussed. However, it remains unclear how much of this recovery behavior was due to continuing cell loss for extended UPC violations and how much was due to network and decoder resynchronization latency. Finally, under noisy channel conditions, impairment of SONET and ATM protocol structures was the primary cause of faltering video quality. The M-JPEG protocol was relatively robust and performed well until network synchronization was lost.

ACKNOWLEDGMENT

Likening to my journeys through commissioning and learning to fly, earning an advanced degree in engineering was an elusive goal that challenged me to the depths of my ability. Accordingly, my first debt of gratitude and praise is for Jesus, our lord for giving me the stamina and capacity to achieve this goal. I am sincerely and continually thankful to God for revealing His creations to us through science.

For my wife, Pamela, I have the utmost respect and admiration for your strength, love, tolerance, and support, which enabled me to focus intensely on the work at hand. You have always been the foundation of our family and the communities in which we live. Your work enhances and accelerates our victories in life and we are each truly grateful for your love.

Caleb, Creghton, Grace, and Emma-Faith – you bring joy into every day of my life. I am thankful to you for the unconditional love you express and for bringing purpose to my life. You have taught me much about the priorities and richness of living a Godly life.

I would like to earnestly thank Professors John McEachen and Murali Tummala for their generous support and sage guidance throughout the thesis process. They have each set the standard for rigorous professional achievement while remaining accessible to students and practical in their perspective toward technology. My passion for engineering has flourished through my experiences with them.

THIS PAGE INTENTIONALLY LEFT BLANK

I. INTRODUCTION

A. BACKGROUND

As the United States Navy moves toward a network-centric philosophy of operations, wide area network video applications will become critically important at the operational and tactical levels of warfare. Accelerated decision cycles and radical changes to traditional organizational structures will demand detailed intelligence products and immediate multi-node conferencing in support of modern warfare operations. Therefore, the behavior of information networks and video applications when constrained by various limitations is of increasing interest in the development of naval information systems. These limitations include network resource constraints, system configuration options, and extrinsic environmental conditions, such as distance and channel noise. This thesis explores some of these limitations and their effect on perceived video quality using commercially available off-the-shelf equipment and software.

High quality, live video is the most demanding network application due to its inherently high bandwidth and low delay requirements. Asynchronous Transfer Mode (ATM) addresses these requirements by providing high-throughput, bandwidth-managed links capable of delivering video data within the unique Quality of Service (QoS) constraints specified by individual users.

The quality of a network application is largely a matter of perspective depending on the specific expectations of each individual consumer. For instance, a consumer who is only interested in data applications puts a very high priority on the guaranteed receipt of every data element. To a certain extent, network latency and delay variation are of little concern as long as the application provides error-free access to data resources within a reasonable amount of time. On the other hand, consumers who are interested in video applications automatically presume that a certain amount of information will be lost or thrown away as a matter of course. In fact, this propensity to discard information starts in the digital sampling process well before the video is ever introduced to a communications

network. In this case, the properties of the Human Vision System (HVS) are exploited to allow the exclusion of information with a resultant savings in required transmission bandwidth. However, compressed digital video applications are acutely sensitive to disruptions or perturbations in the flow of their data. Therefore, the network must provide a higher standard of service in this area for video applications.

Video streams naturally generate very large amounts of data, which can easily exceed the available bandwidth in a network link. The Motion JPEG (M-JPEG) video compression scheme is popular in networked video applications due to its compression efficiency and the inherent error resilience properties of intra-frame encoding. In an intra-frame coded scheme, errors within a video frame do not propagate to subsequent frames. Additionally, M-JPEG video frames can be accessed arbitrarily throughout the sequence without regard to any inter-frame anchoring scheme.

Within an intra-frame video compression scheme, such as M-JPEG, scenes with limited action or detail compress very well and require a relatively small bandwidth allocation. However, as scene complexity increases, the bit rate required for transmission will rise sharply due to the increased entropy of the frame's data. Even at lower frame rates and resolutions, it is possible for the instantaneous data rate to be very high. [2] For this reason, it is difficult to determine exact bandwidth requirements for a particular video stream at the time of connection setup.

This leads to the issue of bandwidth management. Allocating bandwidth according to peak requirements is an inefficient use of network resources. Yet, allocating too little bandwidth will degrade the overall quality of the application. Under its QoS rubric, the ATM Traffic Management Specification 4.1 [3] provides several tools and algorithms to manage the limited bandwidth resource. Some of these QoS functions aim to distribute bandwidth efficiently while others seek to minimize network congestion. In any case, a video stream that violates the agreed upon QoS contract will ultimately suffer cell loss.

Since video is a time-sensitive application, ATM cell loss rate (CLR) will obviously play a critical role in the perceived quality of a decoded video stream. CLR can depend on a number of factors including the physical media, switching techniques, buffer sizes, the number of switches traversed, and the QoS class used for the connection. Since ATM cell loss is often a result of congestion in the switches, prudent selection of appropriate rate control mechanisms can minimize CLR. [8]

B. OBJECTIVES

Given the importance of networked video applications within the context of future naval information systems, this thesis analyzes the performance of a commercially available intra-frame coded video application under various network constraints. It seeks to understand the effects of the following variables on the perceived quality of the application:

- User-accessible M-JPEG encoding parameters
- User-selectable ATM QoS parameters
- Simulated delay and delay variation
- Noise

As a concurrent objective of this work, a packet video experimentation module was developed within the Advanced Networking Laboratory. This laboratory module will serve as a network application testbed for various electrical engineering courses as well as a practical testing environment for future experimental work.

C. RELATED WORK

Various well-known networking and signal processing groups are conducting extensive background research related to this thesis.

The ATM Forum (<http://www.atmforum.com>) is an industry-sponsored consortium dedicated to developing and promoting ATM technology in the marketplace. Under the auspices of this group, numerous committees are actively researching topics covering every aspect of ATM network communications. Beyond the essential protocol

and physical component research done in this forum, topics explored by the Traffic Management Committee are most relevant to this thesis.

In the digital signal processing (DSP) field, the International JPEG Committee (<http://www.jpeg.org>) is an industry-sponsored organization responsible for research and development of the JPEG image compression scheme. This scheme consists of several operating modes; the sequential, or baseline, mode is extended to video as M-JPEG. Within the JPEG Committee, significant new work is underway to develop a wavelet-based image compression scheme known as JPEG-2000. This new scheme will provide improved image compression, enhanced error resilience, and convenient multi-resolution properties. Combined with third generation cellular communication technology, many new possibilities are on the horizon for robust JPEG-2000-based wireless video applications.

While many significant improvements are being made to the related underlying technologies, this thesis focuses on the practical analysis of video quality in commercial implementations of current technology. In this vein, interesting work is also being conducted within similar laboratories around the world.

The Laboratory of Telecommunication Technology at Helsinki University of Technology (<http://www.hut.fi/English/>) is a testing platform for new network applications. The network, codec, and analysis equipment located in this laboratory is very similar to the system developed in this thesis. Some of the work performed in this laboratory includes analysis of software version compatibility issues, ITU-T standard compliance, and efficient integration of real time and non-real time network services. [15]

The German National Research Center for Information Technology, Media Communication Institute (<http://imk.gmd.de/>) is involved in a Distributed Video Production project with ATM technology at its core. [16] This project studies video production where the required cameras, recorders, switches, mixers, and other equipment are located at geographically diverse sites linked by high-bandwidth network connections. Substantial components of the Distributed Video Production project include distributed

virtual studios, distributed telepresence, distributed virtual reality, and distributed video archiving. Delay and its effect on live video production over a distributed network are the primary research concerns in this laboratory. While the core network technology employed in the Distributed Video Production project is similar to the equipment used in this thesis, the scope of the project as well as the broad variety of photographic and DSP equipment are quite different.

D. THESIS ORGANIZATION

This thesis is organized into six chapters and two supporting appendices. Chapter II provides an overview of the relevant aspects of ATM. Chapter III explains the Joint Photographic Experts Group (JPEG) Standard for Still Image Compression. Chapter IV presents both the features of the private ATM network over which the study was conducted and the basic features of ADTECH™'s AX/4000 ATM test system. Chapter V explains experimental procedures and presents results. Chapter VI summarizes the findings of this analysis and wraps up with recommendations for further research. Appendix A details the timelines for the video clips used in this thesis. Finally, Appendix B discusses the procedure for programming the SX/14 Data Channel Simulator to induce cell delay variation.

THIS PAGE INTENTIONALLY LEFT BLANK

II. ATM OVERVIEW

A. INTRODUCTION

Asynchronous Transfer Mode (ATM) is a high-bandwidth switching and multiplexing technology that combines the benefits of circuit switching and packet switching. Using the advantages of both switching technologies, ATM ensures minimum transmission delay and guaranteed bandwidth for circuit switching applications while also providing efficient handling of intermittent traffic for packet switching applications. In addition to traditional data transfer applications, ATM networks are often employed for multimedia and video conferencing applications requiring both high bandwidth and guaranteed QoS.

ATM is a connection-oriented protocol which means that user information travels the network through a pre-established path between two ATM endpoints. ATM supports two types of network connections, Permanent Virtual Connections (PVC's) and Switched Virtual Connections (SVC's). A PVC is a logical connection between two ATM peers that is established to satisfy a standing need for network services. These static connections will remain in service until changed by the user. User applications that require an on-going, specific level of transmission bandwidth typically use PVC's for connectivity. A SVC is a switched connection that is established by means of a defined and standardized ATM signaling protocol. These types of connections are created dynamically as required by the user. SVC data transfers ordinarily occur by means of shared network facilities, rather than through dedicated transmission lines.

ATM cell transmission is asynchronous in nature; traffic without delay constraints can be freely intermixed with time-sensitive traffic through a statistical multiplexing scheme. The fixed sized of ATM cells enables them to be switched through the network by means of high-speed hardware. The fixed-length also prevents a single user from monopolizing the communications channel and thereby crowding out other network users.

B. ATM PROTOCOL REFERENCE MODEL

ATM protocol elements correspond with the lower four layers of the International Standards Organization Open Systems Interconnect (ISO/OSI) model. The ATM protocol provides interface specifications for transferring data between the user and the physical media necessary for communication between geographically separated network nodes. By handling the lower tiers of the OSI model, ATM provides interoperability with existing network architectures and enables integration of multiple traffic formats over a single high-speed network.

Although the ATM protocol reference model is patterned after the OSI reference model, it differs in that it consists of three planes: the control plane, the user plane, and the management plane as shown in Figure 2-1. The functions of these planes, which operate across all four layers of the ATM architecture, are now briefly summarized.

The user plane provides for the transfer of end-user information through the network. This plane is concerned primarily with the ATM layer and the physical layer - the layers most relevant to accomplishing cell relay services in an ATM network.

The control plane provides control functions essential to ATM switched services. It exchanges signaling information between ATM endpoints in order to accomplish connection setup. It handles the processes necessary to set up, manage, and release SVC's between communicating peers in the network.

The management plane performs operations and management functions, as well as information exchange functions between the user plane and the control plane. It accomplishes layer management functions such as detecting failures and protocol abnormalities as well as plane management functions for managing and coordinating the overall ATM architecture.

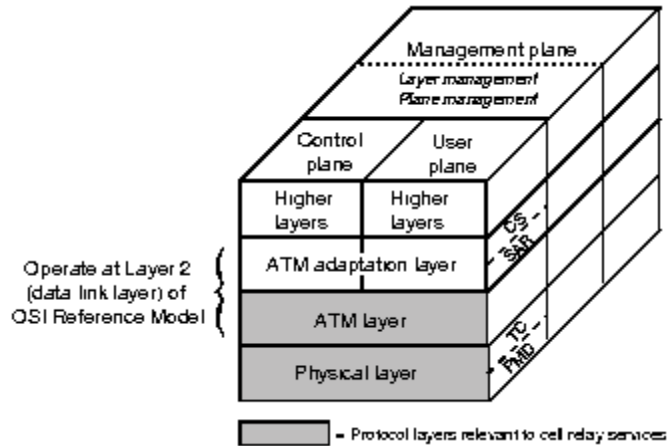


Figure 2-1. ATM Protocol Reference Model from Ref. [1].

The four layers comprising the ATM architecture are briefly summarized below.

- **Higher Layer Applications and Protocols** - These layers relate to specific user applications deployed in the ATM networking environment. These applications could include traditional TCP/IP data transfer, video teleconferencing, etc.
- **ATM Adaptation Layer (AAL)** - The AAL insulates application layer protocols from the details of ATM. At the source, it translates user data received from higher layer protocols into ATM cell payloads. At the destination, it translates ATM cells received from the network and arranges the data in a suitable format for presentation to higher layer protocols. Two service-specific layers within the AAL, the convergence sublayer (CS) and the segmentation and reassembly (SAR) sublayer, perform application-dependent traffic processing.
- **ATM Layer** - The ATM layer operates in conjunction with the physical layer to relay cells from one ATM connection in the network to another. It also coordinates the transmission of data in fixed-size cells and performs the task of multiplexing the various logical connections.

- **Physical Layer.** The physical layer provides the ATM layer with access to the network's physical transmission media, such as a fiber-optic cable or coaxial cable. The process of placing ATM cells onto the physical transmission media takes place in two sublayers of the physical layer: the Transmission Convergence (TC) sublayer and the Physical Medium Dependent (PMD) sublayer. The TC sublayer maps the ATM cell stream to the underlying framing mechanism of the physical transmission medium and generates the required ATM protocol information for the physical layer. The PMD sublayer adapts the ATM cell stream to the specific electrical or optical characteristics of the physical transmission medium. These characteristics include such factors as timing, power, and jitter. [1]

C. ATM SWITCHING

ATM cells are transported to their destinations by means of virtual connections established between communicating network endpoints. Such connections are set up through the exchange of appropriate messaging and routing protocols. Once a connection is established, ATM cells are routed through the network in the same sequence as they were generated.

All traffic to or from an ATM network is prefaced with a Virtual Path Indicator (VPI) and a virtual channel identifier (VCI). A VPI/VCI pair identifies a single virtual circuit (VC) in an ATM network. A VC is a logical circuit created to ensure reliable communications between two endpoints in an ATM network. Each VC constitutes a private connection to another ATM node. A VC is treated as a point-to-point path for unidirectional traffic flows and each VC is considered a separate and complete link to a destination node.

The Virtual Path (VP) is a generic designation identifying a bundle of VCs that are directed to the same ATM endpoint. A VP is identified solely by the VPI field in the ATM cell header (see Figure (2-2)) and can be thought of as a large pipe containing a logical grouping of virtual connections between two ATM endpoints.

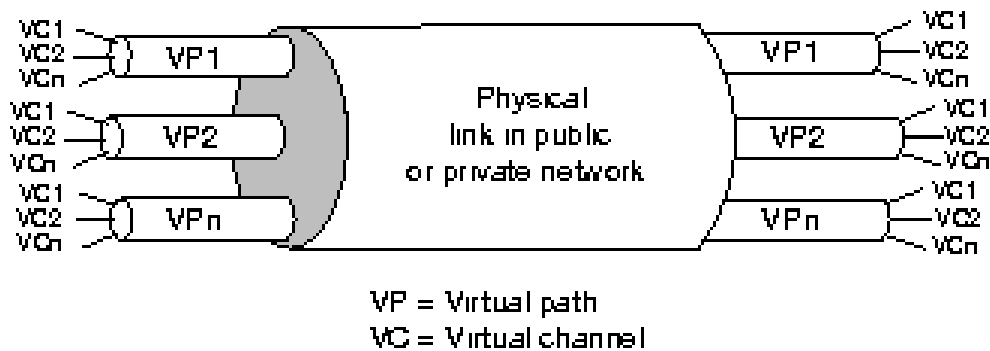


Figure 2-2. Virtual Channels within Virtual Paths from Ref. [1].

An ATM switch accepts a cell from the transmission medium, performs a validity check on control information contained in the cell header, reads the address from the header, and forwards the cell to the next link in the network. The switch immediately accepts another cell that may be part of an entirely unrelated message and repeats the process.

D. ATM TRAFFIC MANAGEMENT

A traffic management regime has been defined to ensure that limited network resources are allocated fairly and QoS objectives are met for both existing and new connections. Traffic management consists of traffic control and congestion control. The primary goal of traffic control is to avoid congestion by dealing with current traffic situations, while congestion control tries to prevent sources' from exceeding available network resources and thereby minimizes network congestion.

1. ATM Service Architecture

The five basic service categories specified in the ATM Forum Traffic Management Specification (Ver. 4.1) are listed below. These service categories relate traffic characteristics and QoS requirements to network behavior at the ATM layer.

- **Constant Bit Rate (CBR)** – CBR is a bandwidth-guaranteed service class and requires a Peak Cell Rate (PCR) definition when the connection is made. The system guarantees bandwidth allocation at the PCR for the duration of the connection. CBR is employed where traffic is time-

sensitive in nature and requires tightly-constrained delay variation (e.g., audio and video applications).

- **Variable Bit Rate (VBR)** – VBR is a more flexible bandwidth-guaranteed service class. The system guarantees a sustained bandwidth allocation for the duration of the connection and makes provisions for maximum peak bandwidth deviations above this allocation. A VBR contract is defined by specifying PCR, Sustainable Cell Rate (SCR), and Maximum Burst Size (MBS) parameters. VBR is employed for bursty traffic that is time-sensitive in nature (e.g., compressed video).
- **Unspecified Bit Rate (UBR)** – UBR is a “best effort” service class and provides no guarantee of bandwidth to the connection. The connection is limited to whatever bandwidth is available at a given point in time. No numerical commitments are made with respect to cell loss or delay parameters. UBR is employed where traffic is not time-sensitive in nature.
[2]
- **Available Bit Rate (ABR)** – ABR is an adaptable service category for which the limiting network transfer characteristics may change subsequent to connection establishment. A flow control mechanism supports several types of feedback that control the source rate in response to changing network conditions. ABR service does not limit the delay or delay variation for a given connection and, therefore, is not intended to support real time applications. An ABR contract is defined by specifying a required PCR and a Minimum Cell Rate (MCR). (Note, the MCR may be set to zero.) During the course of the connection, the bandwidth available from the network may vary, but will never go below the MCR.
- **Guaranteed Frame Rate (GFR)** – The GFR service category is designed for non-real-time applications that may require a minimum cell rate guarantee and can benefit from additional bandwidth dynamically

available in the network. The service guarantee is based on AAL-5 PDUs (frames) and, under congestion conditions, the network attempts to discard complete PDUs instead of discarding cells without reference to frame boundaries. There are no delay bounds associated with this service category and it does not require adherence to a flow control protocol. [3]

2. ATM Quality of Service

When a connection is created across an ATM network, it is possible to specify a QoS that describes the requirements of the traffic on the connection. Through a variety of traffic management techniques, the ATM network can guarantee several differing levels of service to various connections depending on their established QoS contracts.

ATM QoS is measured by a set of parameters characterizing the performance of an ATM layer connection. These QoS parameters quantify end-to-end network performance. Six QoS parameters that correspond to network performance objectives are identified in ATM Forum Traffic Management Specification. [3]

The following QoS parameters are negotiated at the time of connection setup:

- **Cell Delay Variation (CDV)** – The CDV is primarily affected by the switching architecture, buffer capacities, number of tandem nodes in a path, and the total traffic load on the physical connection. Two measurement methods are defined for CDV – one-point CDV and two-point CDV. The negotiated objective for CDV performance is expressed in terms of peak-to-peak CDV. The QoS parameter CDV should not be confused with the connection traffic parameter CDVT. [3]
- The one-point CDV describes variability in the pattern of cell arrivals at a single measurement point with reference to a negotiated peak arrival rate. Positive values of the one-point CDV correspond to cell clumping while negative values correspond to gaps in the cell stream. [3]

- The two-point CDV describes variability in the pattern of cell arrivals at the output of a connection portion with reference to the pattern of the corresponding arrivals observed at the input to the connection portion. [3]
- **Cell Transfer Delay (CTD)** – The CTD between two measurement points is the sum of the total inter-ATM node transmission delay and the total ATM node processing delay. These delays include propagation, queuing, routing, and switching delays. [3]
- **Cell Loss Ratio (CLR)** – CLR is an end-to-end dependability parameter. ATM management plane functionality is used to record the number of cells transmitted and received on a connection. The difference, cells transmitted minus cells received, can then be calculated. If this difference is positive, the CLR is then calculated as the ratio between this difference and the actual number of cells transmitted. If this difference is negative, an instance of cell misinsertion (see below) may have occurred. The CLR is primarily affected by errors in the cell header, buffer overflows, and non-ideal Usage Parameter Control (UPC) actions. [3]

The following QoS parameters are not negotiated:

- **Cell Error Ratio (CER)** – The CER is the ratio of errored cells to the sum of successfully transmitted cells plus errored cells transmitted over a connection. Errored cells are defined as those cells received where the binary content of their payload differs from that of the corresponding transmitted cell payload or the cell is received with an invalid header field after header error control procedures are completed. The CER is primarily affected by the error characteristics of the physical media. [3]
- **Severely Errored Cell Block Ratio (SECBR)** – The SECBR is the ratio of severely errored cell blocks to the total number of transmitted cell blocks. A cell block is a sequence of N cells transmitted consecutively on a given connection. A severely errored cell block occurs when more than

M errored cells, lost cells, or misinserted cells are observed within a received cell block. For practical purposes, a cell block normally corresponds to the number of user information cells between successive Operation and Maintenance (OAM) cells. The SECBR is primarily affected by the error characteristics of the physical media and by buffer overflows. [3]

- **Cell Misinsertion Rate (CMR)** – The CMR is the ratio of misinserted cells per time interval, T_m . ATM management plane functionality is used to record the number of cells transmitted and received on a connection. The difference, cells received minus cells transmitted, can then be calculated. If this difference is positive, the CMR is then calculated as the ratio between this difference and the measurement time interval, T_m . Otherwise, an instance of cell loss may have occurred during T_m . Cell misinsertion on a particular connection is primarily caused by an undetected error in the header of a cell being transferred on a different connection. [3]

3. ATM Traffic Contract

A traffic contract is negotiated between the user and an ATM network at connection setup time. It is defined as an implicit agreement between the ATM end user and the network, which includes connection traffic descriptors, a requested QoS class, and a conformance definition [4]. In general, QoS conformance definitions are distinguished by the manner in which a connection's QoS parameters, particularly CLP, apply to high priority (CLP=0) or total (CLP=0+1) cell flows. Under this scheme, a cell is described as "marked" when its originator has set the CLP bit to "1" in the ATM cell header; a cell is described as "tagged" when a network device has set the CLP bit to "1" in the ATM cell header.[3] In other words, the CLP=0 cell flow contains cells that were not designated as cell drop candidates by their originator; nor have they been found non-conforming by a network entity. The CLP=0+1 cell flow is the aggregate flow of cells.

A traffic source's inherent characteristics are described by the various traffic parameters listed below. For a given connection, these traffic parameters make up a *source traffic descriptor*, which becomes part of the broader *connection traffic descriptor*.

- **Peak Cell Rate (PCR)** – An upper bound on the traffic that can be submitted on a connection.
- **Sustainable Cell Rate (SCR)** – An upper bound on the conforming average of an ATM connection.
- **Maximum Burst Size (MBS)** – The maximum number of consecutive cells that a connection can accept traffic at the peak cell rate. This parameter implies a maximum burst time for any instantaneous cell rate. [5]
- **Burst Tolerance (BT)** – The largest burst of data that a network device is guaranteed to handle without discarding cells. The Burst Tolerance is conveyed through the MBS, which is coded as a number of cells. The BT, along with the SCR and the GCRA determine the maximum time that a circuit can transmit at its PCR before falling out of conformance. [5]
- **Minimum Cell Rate (MCR)** – A lower bound on the traffic that can be submitted on a connection.
- **Maximum Frame Size (MFS)** – An upper bound on the size of an AAL-5 protocol data unit under the GFR service category.

The source traffic descriptor is used to capture an ATM source's intrinsic traffic characteristics during connection establishment. The connection traffic descriptor specifies the traffic characteristics of the ATM connection. It includes the source traffic descriptor, the Cell Delay Variation Tolerance (CDVT), and the conformance definition for a specific QoS category. [3]

A QoS conformance test is applied to cells as they pass through the user-network interface (UNI). Cell conformance is evaluated with respect to a negotiated QoS contract.

Conformance definitions for CBR, VBR, and UBR connections are based on the results of one or more instances of the Generic Cell Rate Algorithm (GCRA). The ABR conformance definition only applies to high-priority cell flows. It is implemented through feedback received from Resource Management (RM) cells. The GFR conformance definition only applies to cells of frames designated as eligible for service. GFR conformance is characterized by the PCR, CDVT, and MFS parameters as well as consistent CLP bit values for cells within a frame. However, for all of these service categories, precise definitions of compliant connections are unique to each particular network. [3] For the purposes of this study, only CBR and VBR connections will be considered.

4. Traffic Contract Parameters and Related Algorithms

a. Cell Delay Variation Tolerance for PCR and SCR

Cell delay variation tolerance represents an upper bound on the peak-to-peak variation in cell inter-arrival times. This peak-to-peak variation is also known as “cell clumping” because cells are not arriving at a uniform rate. The variation is primarily caused by queuing delays due to the cell multiplexing process or management (system overhead) cell insertions. Video compression is another secondary cause of cell delay variation in multimedia networks. Large peak-to-peak variations can cause excessive cell clumping which may result in cell losses at the affected node.

b. Generic Cell Rate Algorithm

Conformance tests for CBR, VBR, and UBR are based on a continuous state Leaky Bucket algorithm known as the Generic Cell Rate Algorithm. Conceptually, the Leaky Bucket algorithm is seen as a bucket with a fixed-size hole at the bottom, draining its content at a constant rate. As cells arrive, they are placed in the bucket. If too many cells arrive in a short period of time, an overflow occurs and those cells regarded as non-compliant will be either tagged or dropped according to the UPC in force for that connection.

The GCRA is used to define the relationship between PCR and CDVT and the relationship between SCR and Burst Tolerance (BT) using two parameters: the

increment (I) and the limit (L). Several different instances of the GCRA may be applied to one or multiple flows of the same connection with possibly different increment and limit parameters. A cell is then considered “conforming” only if it conforms to all instances of the GCRA applicable to its flow. [3] A common multiple GCRA scheme known as Dual Leaky Bucket GCRA is depicted in Figure (2-3).

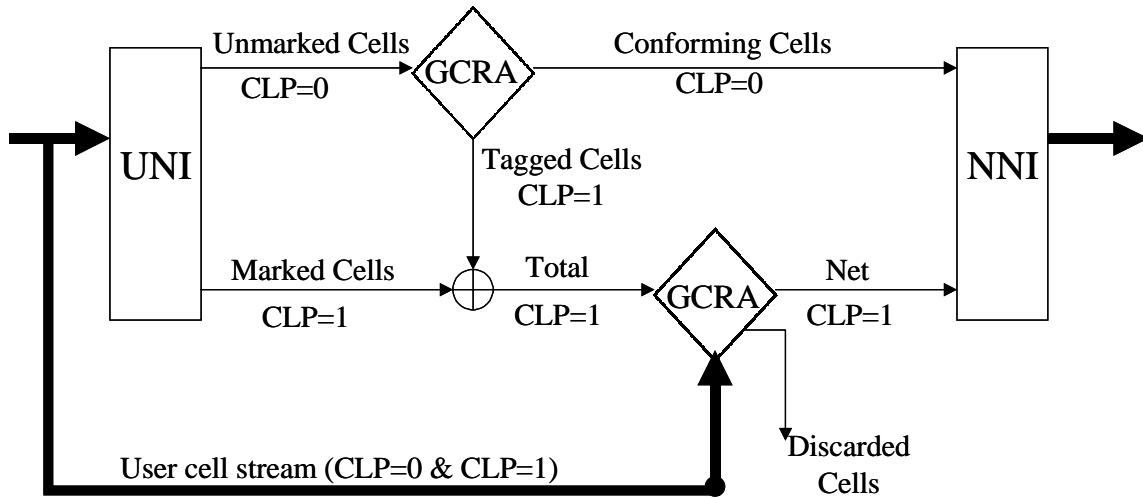


Figure 2-3. Dual Leaky Bucket GCRA from Ref. [6].

5. CBR and VBR Traffic Contract Conformance Definitions

Conformance for a CBR connection is characterized by a PCR and corresponding CDVT for the CLP=0+1 traffic flow. Conformance for a VBR connection is characterized by an SCR and corresponding MBS for one or more traffic flows in addition to a PCR and corresponding CDVT for at least the CLP=0+1 flow. In addition to their QoS parameters, VBR connections are also distinguished by the magnitude(s) of the MBSs they support. Specific conformance definitions for the following QoS service categories are taken from [3].

a. CBR.1: Conformance Definition for PCR (CLP=0+1)

Cell tagging is not applicable to this conformance definition since no separate rate is specified for CLP=0 cell stream. The CLR objective applies to the

aggregate CLP=0+1 cell stream. The following is a conformance definition for a source traffic descriptor that specifies a PCR for the CLP=0+1 cell stream:

- One GCRA(T_{0+1} , CDVT) defining the CDVT in relation to the PCR of the CLP=0+1 cell stream. T_{0+1} is defined as the inverse of the specified PCR cell flow.
- A cell that is conforming to the GCRA above is said to be conforming to this connection traffic descriptor.

b. VBR.1: Conformance Definition for PCR (CLP=0+1) and SCR (CLP=0+1)

Cell tagging is not applicable to this conformance definition. The CLR objective applies to the aggregate CLP=0+1 cell stream. The following is a conformance definition for a source traffic descriptor that specifies PCR for the CLP=0+1 cell stream and SCR for the CLP=0+1 cell stream:

- One GCRA(T_{0+1} , CDVT) defining the CDVT in relation to the PCR of the CLP=0+1 cell stream. T_{0+1} is the inverse of PCR (CLP=0+1).
- One GCRA(T_{s0+1} , $BT_{0+1} + CDVT$) defining the sum of the CDVT and the BT in relation to the SCR of the CLP=0+1 cell stream. T_{s0+1} is the inverse of SCR (CLP=0+1).
- A cell that conforms to both GCRA's above is said to be conforming to this connection traffic descriptor.

c. VBR.2: Conformance Definition for PCR (CLP=0+1) and SCR (CLP=0)

This conformance definition allows a connection to send CLP=1 cells at a PCR equal to the specified PCR of the CLP=0+1 cell stream. The CLR objective applies to the CLP=0 cell stream. CLRs for the CLP=1 cell stream and the aggregate stream are undefined. The following is a conformance definition for a source traffic descriptor that specifies PCR for the CLP=0+1 cell stream and SCR for the CLP=0 cell stream:

- One GCRA(T_{0+1} , CDVT) defining the CDVT in relation to the PCR of the CLP=0+1 cell stream. T_{0+1} is the inverse of PCR (CLP=0+1).
- One GCRA(T_{s0} , BT_0+CDVT) defining the sum of the CDVT and the BT in relation to the SCR of the CLP=0 cell stream. T_{s0} is the inverse of SCR (CLP=0).
- A CLP=0 cell that is conforming to both GCRA's above is said to be conforming to this connection traffic descriptor. Additionally, a CLP=1 cell that is conforming to the GCRA(T_{0+1} , CDVT) above is said to be conforming to the connection traffic descriptor.

d. VBR.3: Conformance Definition for PCR (CLP=0+1) and SCR (CLP=0)

This conformance definition allows a connection to send CLP=1 cells at a PCR equal to the specified PCR of the CLP=0+1 cell stream. The CLR objective applies to the CLP=0 cell stream. CLRs for the CLP=1 cell stream and the aggregate stream are undefined. The following is a conformance definition for a source traffic descriptor that specifies PCR for the CLP=0+1 cell stream and SCR for the CLP=0 cell stream:

- One GCRA(T_{0+1} , CDVT) defining the CDVT in relation to the PCR of the CLP=0+1 cell stream. T_{0+1} is the inverse of PCR (CLP=0+1).
- One GCRA(T_{s0} , BT_0+CDVT) defining the sum of the CDVT and the BT in relation to the SCR of the CLP=0 cell stream. T_{s0} is the inverse of SCR (CLP=0).
- CLP=0 cells conforming to both GCRA's above are said to be conforming to this connection traffic descriptor. CLP=1 cells that conform to GCRA(T_{0+1} , CDVT) above are also said to be conforming to this connection traffic descriptor.
- If the end-system requests tagging, and if tagging is supported by the network, a CLP=0 cell that is not conforming to GCRA(T_{s0} , BT_0+CDVT) above, but is conforming to GCRA(T_{0+1} , CDVT) above, will have its CLP

bit changed to “1” and is said to be conforming to the connection traffic descriptor.

Conformance definitions for other ATM service categories are not applicable to this thesis but may be found in [3].

6. Usage Parameter Control

UPC, or "traffic policing", is defined as the set of actions taken by the network to monitor traffic and enforce the traffic contract. Its main purpose is to protect network resources from malicious as well as unintentional misbehavior, which can affect the QoS of other established connections. This protection is achieved by detecting violations of negotiated parameters and taking appropriate actions.

UPC enforcement actions are intended to ensure conformance with a negotiated QoS traffic contract. Traffic parameters that may be subject to UPC enforcement are those included in the source traffic descriptor. At the cell level, actions of the UPC function may include cell passing, cell tagging, and cell discarding. Cell passing essentially equates to no action, while cell discarding immediately removes a non-conforming cell from the stream. On the other hand, cell tagging may take a more flexible approach based on the current network capacity. In general, the UPC will tag cells that violate the QoS contract rather than pass or discard them. However, these tagged cells are the first to be dropped in the event of network congestion.

Cell tagging operates on CLP=0 cells only. When a CLP=0 cell is found in non-conformance by the GCRA, the UPC takes action by setting the cell's CLP bit to “1”. When no additional network resource has been allocated for the CLP=1 traffic flow, these non-conforming cells may be simply discarded [3]. Otherwise, the CLP=1 flow continues through the next local GCRA iteration or on to the next network node.

UPC is an application-dependent, user-defined function. Therefore, the UPC algorithm itself should not be interpreted as a contract conformance definition. Even though cell conformance is based on the GCRA for CBR, VBR, and UBR traffic, the

network may use any UPC algorithm, as long as it does not violate the QoS objectives of compliant connections. [3]

E. SUMMARY

This chapter provided an overview of the ATM network architecture and its relevance to the work presented in this thesis. ATM concepts and terminology were presented as lead-in material to a discussion of pertinent topics from the ATM Traffic Management Specification. Within the Traffic Management area, various QoS performance definitions, network performance algorithms, and system control tools were presented with respect to their particular functionality or impact on network behavior. The next chapter introduces relevant concepts and background information regarding the Motion JPEG video compression standard and its affect on network performance.

III. MOTION JPEG COMPRESSION

A. INTRODUCTION

Motion-JPEG (Motion - Joint Photographic Experts Group or M-JPEG) is an extension of the joint International Telecommunications Union (ITU) and International Standards Organization (ISO) JPEG standard for continuous tone (multilevel) still images. The JPEG standard specifies several modes of operation including

- **Sequential encoding** - each image component is encoded in a single left-to-right, top-to-bottom scan;
- **Progressive encoding** - the image is encoded in multiple scans for applications in which transmission time is long, and the viewer prefers to watch the image build up in multiple coarse-to-clear passes.
- **Lossless encoding** - the image is encoded to guarantee exact recovery of every source image sample.
- **Hierarchical encoding** - the image is encoded at multiple resolutions, so that the lower-resolution versions may be accessed without first having to decompress the image at its full resolution. [7]

As an extension of the JPEG still image standard, M-JPEG removes only intra-frame redundancy and not inter-frame redundancy. This results in significantly less compression than an inter-frame compression technique would provide. Another drawback of M-JPEG is that audio is not integrated into the compression method. The lack of inter-frame coding can be viewed as an advantage for some video applications or environments. For instance, if direct access to a random video frame is desired, M-JPEG will provide faster and more flexible access than a technique that removes inter-frame redundancy. In an inter-frame coding scheme, only a small portion of the total frames are accessible as stand-alone images. Thus, it may be necessary to wait for multiple frames to arrive before having access to a still frame in the video sequence. [8] Additionally, M-

JPEG may be a more robust encoding scheme than inter-frame compression techniques in error-prone environments because each frame is independent of the frames before and after it. Therefore, an error occurring in a previous frame will not be carried forward to subsequent frames in the video sequence.

B. OVERVIEW OF THE SEQUENTIAL (BASELINE) JPEG COMPRESSION ALGORITHM

Some of the earliest industry attention to the JPEG proposal focused on the baseline sequential codec as a motion (intraframe) image compression method. [7] Figure (3-1) outlines the baseline JPEG compression algorithm.

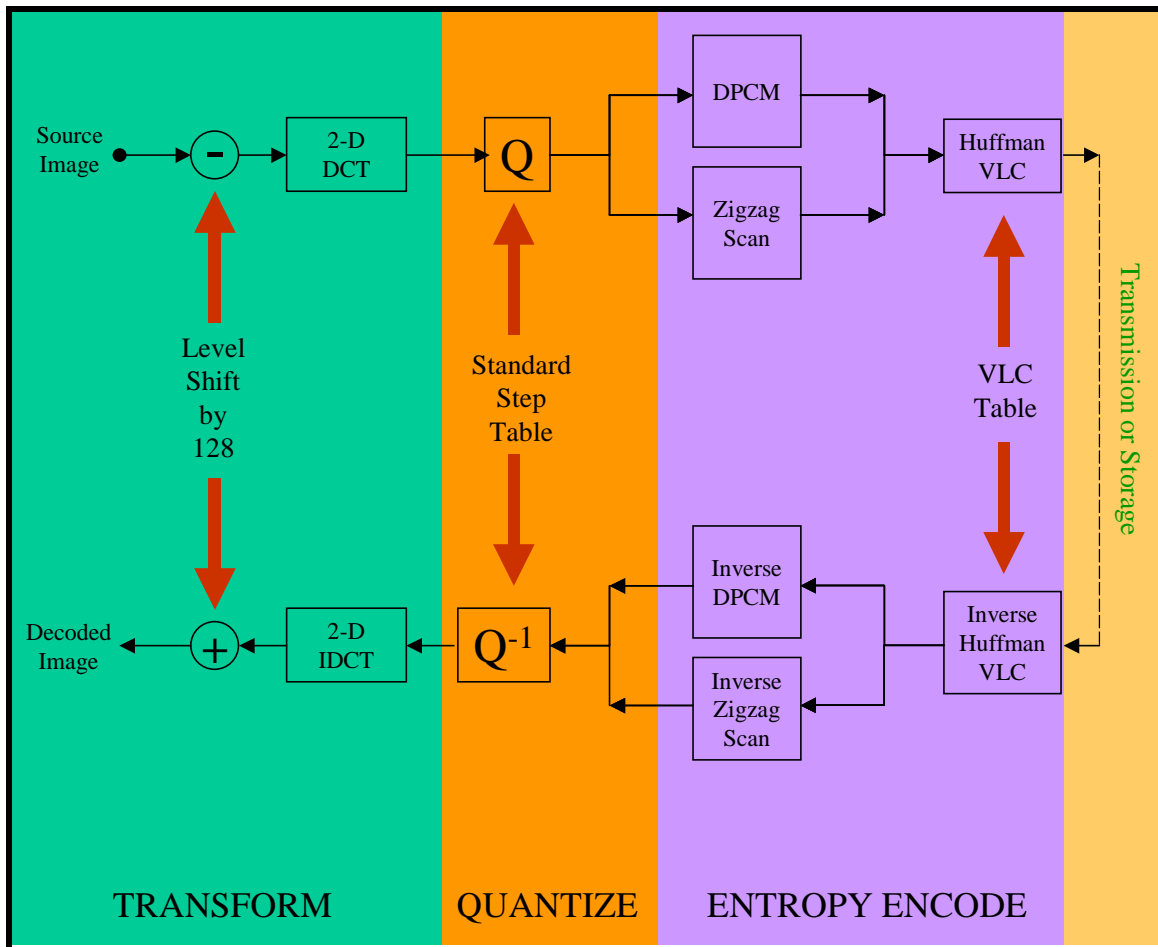


Figure 3-1. Baseline JPEG Codec.

1. Decomposition

The JPEG algorithm is given raw image data in terms of YUV¹ colorspace components with color sample intensity values ranging from 0 to 255. Each component of the original image is divided into 8×8 blocks and these blocks are then processed in row-major order (i.e. blocks in the same row are processed sequentially from left to right). [9] Thus, color image compression on a per-component basis is essentially the same as compressing multiple grayscale images. [7] The component images are either compressed one at a time, or are compressed by alternately interleaving 8×8 sample blocks from each component in turn.

Before performing the transform operation on a block, each element of the block is level-shifted by subtracting 128. This level-shift biases the compression around neutral intensities and thereby aids in compression efficiency.

2. Discrete Cosine Transform

In this step, each block is transformed using the Discrete Cosine Transform (DCT). The DCT can be obtained from the Discrete Fourier Transform (DFT). [10] However, whereas the normal DFT introduces spurious high frequency components because of its forced periodicity, the DCT avoids this distortion by mirroring the N-point data sequence prior to transforming it. A 2N-point DFT is then calculated and the first N points of this transformed sequence become the DCT sequence. In this case, forced periodicity will not produce any sharp discontinuities in the time series and spurious high frequency components will not appear in the transform domain. Thus, the transformed block has its signal energy concentrated in the lower-order coefficients. The (0,0) element of the transformed block is called the DC Component, and the other 63 elements are referred to as the AC Components. [9] The DCT is obtained through the relationship

¹ The YUV colorspace includes one luminance (Y) and two chrominance (U,V) components. YUV is related to the RGB colorspace by a linear translation of the components. However, YUV values do not always map to legitimate RGB coordinates. Most computer terminals receive video input as RGB components so these anomalies will adversely affect display quality. Therefore, most JPEG applications use the YC_rC_b colorspace, a derivative of YUV, where C_r specifies the redness of the image and C_b specifies the

described by Equation (3.1). In Equation (3.1), Y is the resultant DCT coefficient matrix given the input image, X, which measures N_m pixels vertically and N_n pixels horizontally.

$$Y(m, n) = \sum_{i=0}^{N_m-1} \sum_{j=0}^{N_n-1} 4 \cdot X(i, j) \cdot \cos\left[\frac{\pi \cdot m}{2 \cdot N_m} \cdot (2 \cdot i + 1)\right] \cdot \cos\left[\frac{\pi \cdot n}{2 \cdot N_n} \cdot (2 \cdot j + 1)\right] \quad (3.1)$$

3. Quantization – Scaling and Rounding

Quantization is a many-to-one mapping, and is, therefore, a fundamentally lossy process. In fact, it is the principal source of lossiness in DCT-based encoders. [7]

As shown in Equation (3.2), each of the 64 coefficients in the transformed block is divided by its corresponding element in an 8×8 quantization table, Q_{uv} . The scaled coefficients are then rounded to the nearest integer. [9] This quantization procedure eliminates perceptually unimportant coefficients in preparation for lossless entropy coding. Additionally, q_s , also known as the Q-Factor, can be adjusted to provide greater compression at the cost of image quality. As a default, the value of q_s is 16; increasing q_s above the default value increases the compression ratio.

$$F_q(u, v) = \text{round}\left(\frac{F(u, v) \times 16}{Q_{uv} \times q_s}\right) \quad (3.2)$$

The selection of a suitable Q-Factor is one of the major variables affecting networked video performance and image quality. Much of this thesis is devoted to the analysis of these effects.

4. Entropy Coding

Quantization tends to produce large blocks of zeros in the higher frequency elements of the transformed block. In preparation for the entropy encoding process, each quantized 8×8 block is converted to a 64-element vector using a fixed one to one mapping as shown in Figure (3-2).

blueness of the image. This guarantees a valid mapping into the RGB colorspace for image display.

quantization block. This block is multiplied by the QT and the Inverse DCT (IDCT) is applied. [9]

C. COMPRESSION AND PERFORMANCE

M-JPEG develops a variable amount of compression for each video frame depending on the characteristics of the image being processed. A complex image will not compress as well as a simpler image. [2] Therefore, as the characteristics of a video sequence change temporally, the required bandwidth of an M-JPEG compressed video stream may become highly variable or “bursty”.

Within a video frame, image quality is controlled by adjusting the Q-Factor parameter. Lower Q-Factor values cause less information loss during the compression process and produce a better quality image at the cost of a higher bandwidth requirement. Higher Q-Factors produce progressively lower quality video. Whenever information is lost due to the JPEG compression algorithm, visual artifacts are established in the resulting image. These artifacts are most prevalent as “ringing” around sharp edges within the image. [2] As the Q-Factor is further increased, an additional “blocking” artifact appears as a result of the block-based DCT implementation.

Since bandwidth is a limited resource, compression of video streams is assumed for most applications. Looking at the instantaneous bandwidth requirement of a compressed video sequence, one can see that burstiness can be very problematic. On the one hand, allocating a constant bandwidth to a compressed video source based on its peak requirements will result in an inefficient use of network resources. On the other hand, managed bandwidth schemes may sacrifice the perceived quality of a video stream if its temporal burstiness exceeds the specifications of a negotiated QoS contract. These competing concerns must be balanced with due consideration for the additional effects of channel noise in order to provide an affordable service at an acceptable level of quality.

D. SUMMARY

This chapter presented a technical overview of the JPEG still image compression standard as extended to M-JPEG for video applications. Primary consideration was given

to the sequential, or baseline, encoding mode of operation since this mode is implemented by the video codec used in this work. The various steps of the algorithm were briefly outlined as background information to the experimental portion of this thesis. Finally, the effects of compression on image quality and bandwidth variability are discussed. These issues will be explored in detail in Chapter V. The next chapter specifies the video and networking equipment and explains the basic organization of the experimental network used in this thesis.

THIS PAGE INTENTIONALLY LEFT BLANK

IV. EQUIPMENT OVERVIEW

A. AVA-300 VIDEO/AUDIO ENCODER

The Marconi Systems StreamRunner™ AVA-300 is a stand-alone encoding platform for one-way video and audio multicast applications. The AVA-300 receives video and audio signals from conventional analog sources, digitally samples these signals, and converts them to ATM Adaptation Layer 5 cells for direct transfer over an ATM network. The AVA-300 interfaces with the network through a 155 Mbps multimode fiber (SC) connection. The ATM network can then be used to switch or multicast the video and audio to any number of desired locations.

The AVA-300 supports both PAL (50 Hz) and NTSC (60 Hz) video formats for analog video input. Six RCA sockets, configurable as 6 composite channels or 3 S-Video channels, are available for video input. Video inputs may be multiplexed onto a maximum of four output streams. Digital video can be produced in uncompressed 24-bit, 16-bit, or 8-bit RGB or 8-bit monochrome formats. Compressed digital video is produced using M-JPEG video compression. User-selectable JPEG Q-Factors and frame rates are shown in Table (1).

<u>Q-Factors</u>	<u>Frame Rates</u>
20	1 fps
32	2 fps
64	5 fps
128	10 fps
200	15 fps
256	30 fps
512	
1024	

Table 4-1. AVA-300 User-Selectable Motion-JPEG Parameters.

The AVA-300 supports 8-bit and 16-bit Pulse Coded Modulation (PCM), A-Law or μ -law (stereo/mono) audio formats with sampling rates selectable from 5 kHz to 44.1 kHz. There are six RCA input sockets on the front panel equaling three stereo input channels. Only one input channel at a time is selectable for ATM network transmission.

B. ATV-300 VIDEO/AUDIO DECODER

The Marconi Systems StreamRunnerTM ATV-300 is a stand-alone decoding platform for one-way video and audio multicast applications. It interfaces with the ATM network through a 155 Mbps multimode fiber (SC) connection. The ATV-300 receives AAL 5 cells containing digital video and audio signals from an AVA-300 encoder either by direct connection or via an ATM network. The ATV-300 then decodes the digital signals and provides full-frame-rate interlaced video output to a conventional analog device such as a television or VCR.

The ATV-300 supports both PAL (50 Hz) and NTSC (60 Hz) video formats for analog video output through its one S-Video connector or its one RCA/Phono socket for composite output. The ATV-300 also provides two RCA/Phono sockets for stereo audio output. The decoder is capable of concurrent decompression of up to four multiple AVA format Motion-JPEG digital video streams.

User control of the AVA/ATV-300 system is provided through the ATV-300 using a workstation-based software interface or a handheld Infrared Remote Control Unit. In addition to adjusting video, audio, and network parameters, the Infrared Remote Control Unit allows the user to chose between multiplexed and single-stream video/audio modes. Multiplexed mode operation requires LAN emulation in order to configure and control the various input and output options. Operation of the AVA/ATV-300 system in the single-stream mode does not require LAN emulation and can be accomplished entirely with the Infrared Remote Control Unit.

C. ASX-200BX ATM SWITCH

The Marconi Systems ForeRunnerTM ASX-200BX is a non-blocking ATM switch capable of switching 2.5 Gbps on a continual basis. The ASX-200BX switches available

in this laboratory are each equipped with eight 155 Mbps fiber optic ports for a total effective capacity of 1.25 Gbps. Each switch performs Usage UPC traffic policing through a Dual Leaky Bucket implementation of the GCRA. [12]

D. SX/14 DATA CHANNEL SIMULATOR

The ADTECH™ SX/14 models a full-duplex digital communication link for testing and evaluation of network equipment and software. Error and delay parameters on the simulated link are controlled by the user. Errors generated by the SX/14 are statistically independent on a per bit basis. The SX/14 can operate at data rates from 100 bps to 155 Mbps. Channel delays can be set from 0 to 323 ms at 155 Mbps with 1 ms resolution.

The SX/14 inserts binomial-distributed (simulated Gaussian) random bit errors with probabilities of bit error ranging from 1×10^{-12} to 1. Additionally, the system can insert user-controlled random burst errors.

Burst length can be fixed or variable about the mode (most frequently occurring value) of a Rayleigh-distributed random variable. The user specifies the mode of the burst length in terms of milliseconds or number of bits. The resulting mean burst length is approximately 25% larger than the specified mode value and the maximum burst length is 4 times the mode value. Burst density determines the error probability during the length of the burst and can range from 1×10^{-8} to 1.

Gap length determines the amount of time between burst errors. This parameter either can operate randomly or be triggered manually by the user. Random gap lengths are generated by a Bernoulli random process, which results in a geometrically distributed inter-burst gap length. In the random case, the user-defined gap length becomes the mean of the geometric distribution. [12]

User-designed error sequences of up to ninety-nine steps can be programmed into the SX/14. A step consists of a set of parameters that will remain in effect for the duration of the step. These parameters include random or burst error settings, delay, and data rate

with user-selectable step duration from 1 to 9,999,999 seconds. After the last step, the program can either stop or repeat from the beginning.

E. AX/4000 ATM TEST SYSTEM

The ADTECH™ AX/4000 is a rack-mounted, hardware-based test system designed for measuring the performance of ATM networks in real time based on user-defined scenarios. Available performance tests include physical layer testing, ATM transmission QoS testing, network load testing, and live ATM traffic monitoring. The main components of the AX/4000 are the chassis with a General Purpose Interface Bus (GPIB), controller module, external controller, generator/analyzer modules and physical port interfaces (e.g., OC-3c/STM-1 Single Mode, DS3, and OC-12c/STM-4c). The port interfaces provide a physical interface between the ATM physical layer and the AX/4000 modules. Windows-based controller software provides user access to the various setup and test control parameters. [14]

Block diagrams in the user interface show the flow of the signal path being tested. Each block is accessible for parameter changes. System configuration data and measurement results can be saved on disk for further analysis. The captured data can also be exported to the other software processing environments, such as Excel or Matlab. The system components and some of the basic functions will be discussed in the next section.

1. System Window

The AX/4000 software uses the System window to display the port configuration and status summary, and to provide direct access to the generator and analyzer dialog boxes. Arranged by port assignments, there is an LED for each generator, and analyzer present in the system.

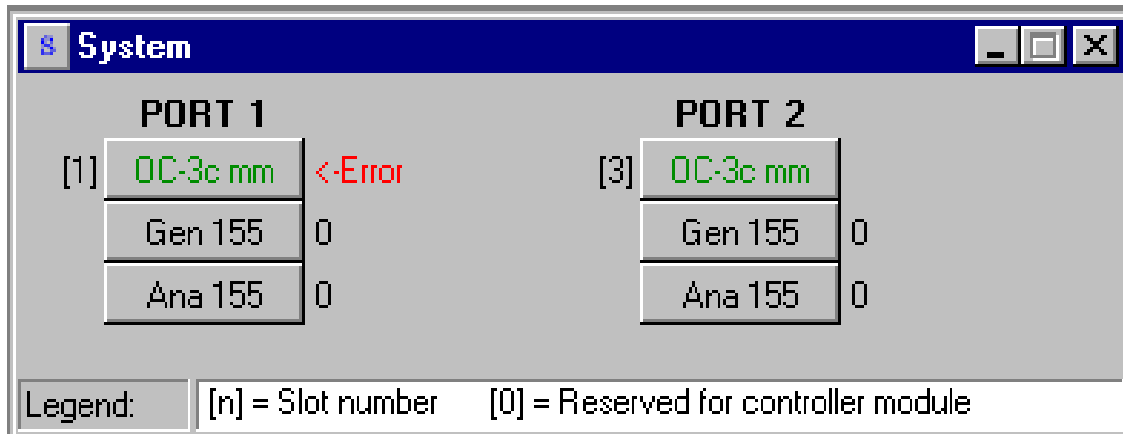


Figure 4-1. AX/4000 System Window.

The interface LED is labeled with the interface type installed on that port. In Run mode, the LED's associated with active modules are colored green; otherwise, they are colored black. A red <-error message appears if any alarms or errors are recorded.

The generator LED is labeled Gen 155 and the analyzer LED is labeled Ana 155. Both LEDs are colored green when the generator/analyzer is running and colored black when stopped. The aggregate assigned cell count of the transmitted/received cells is displayed on the right side of the button. For the generator, the count is displayed in black, but will become blue when at least one of the traffic sources in the generator experiences congestion or runs at full bandwidth. Additionally, the analyzer's count is displayed in black, but will become red when any cell errors are recorded [14].

2. Generator Module

The ATM Generator module creates user-defined cell streams that simulate real traffic patterns. The generator module occupies one chassis slot and provides one port and up to eight programmable traffic sources.

Of the eight sources, seven are foreground traffic sources while one is a background source. When the background source is not used, only unassigned cells will be transmitted while the foreground sources are idle. Otherwise, the background source will transmit user-defined cells when the sources are silent.

Each source and the aggregate stream have a traffic shaper that implements the GCRA. Traffic shaping allows the user to limit the minimum average cell spacing and burstiness of the traffic stream to prevent cell clumping. The shaped, or smoothed, cell stream is expected to conform to a traffic contract based on PCR, SCR, CDVT and MBS. Nonconforming cells are either tagged or dropped depending upon user selection.

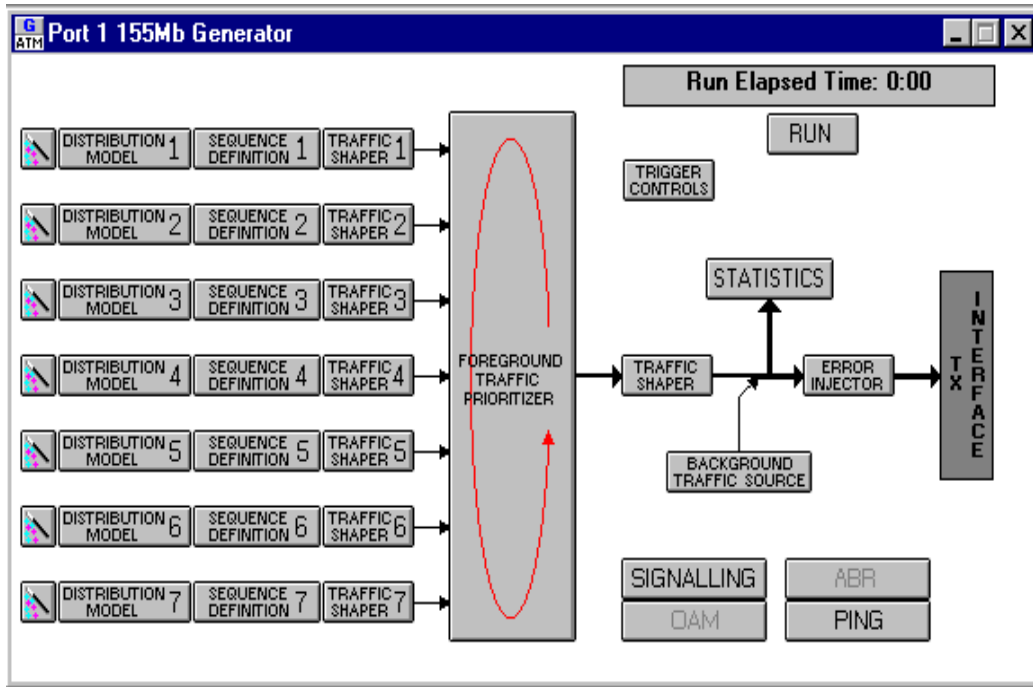


Figure 4-2. AX/4000 Generator Dialog Box.

The foreground traffic prioritizer is used to simulate the effects of different ATM classes of service. The foreground sources may have one of the four priority modes simulating one, two, three, or seven classes of service. The background source is always assigned the lowest priority.

3. Analyzer Module

The analyzer module monitors the traffic stream, provides QoS measurements and statistics, and displays the raw data being carried. The measurements include aggregate cell count, uncorrected header error count, and corrected header count.

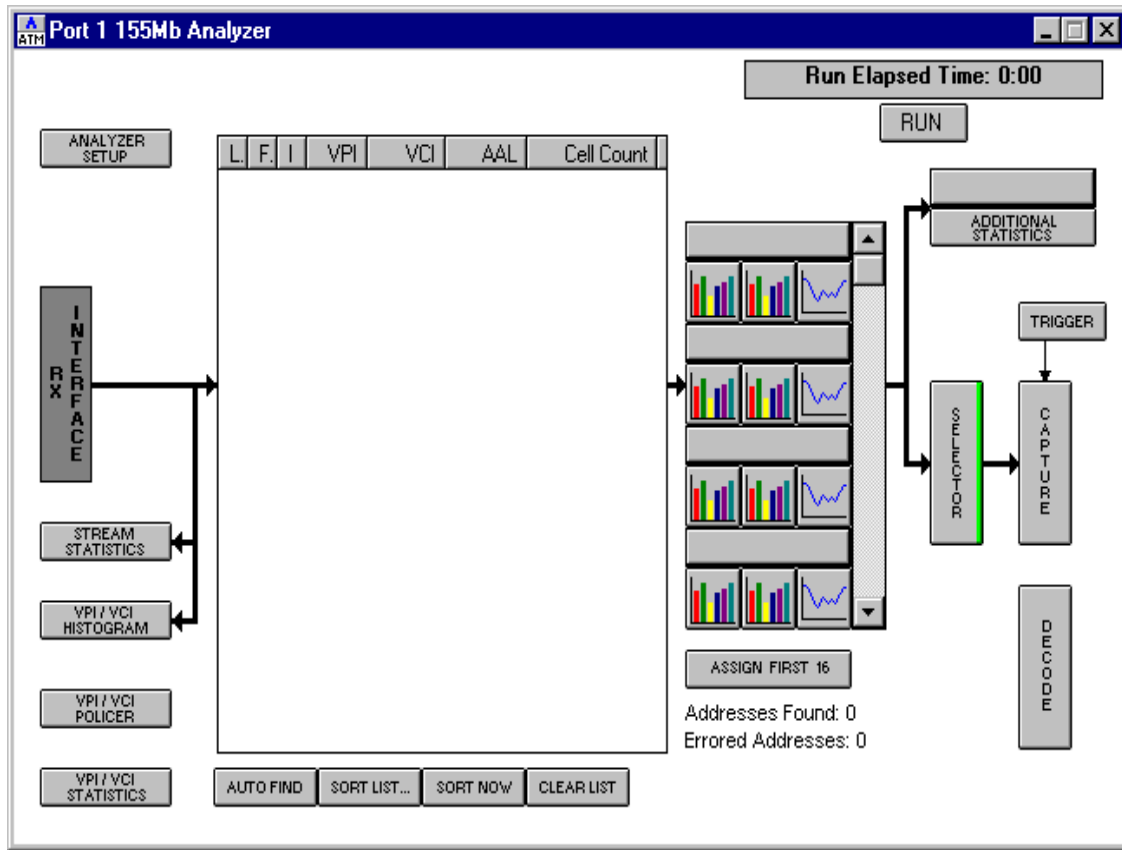


Figure 4-3. AX/4000 Analyzer Dialog Box.

In addition to these composite cell stream measurements, the analyzer module provides 16 cell filters, which can be configured to divide the composite traffic stream into separate substreams for detailed analysis.

The cell capture function provides full-rate cell or header-only capture options for more detailed analysis. The captured cells can be from any combination of the 16 substreams or non-captured cell streams such as unassigned cells. Captured cells can be reassembled and saved to a file for retransmission in any of the foreground or background sequences. Cell capture can be triggered both manually and by an event, such as matching a specific error mask, exceeding peak cell rate thresholds, or non-compliant cell occurrences. Captured cells can also be decoded to provide detail about the content of specific traffic.

In addition to numerical data, the analyzer can also generate histograms for each substream based on Cell Transfer Delay, Cell Inter-arrival Delay, Cell Loss Count, Congestion ratio, and many other QoS measurements.

For each substream, traffic policing can be applied to the incoming traffic stream to test traffic contract compliance.

F. SUMMARY

This chapter described the specifications of each major piece of equipment used in the Advanced Networking Laboratory's Video Testing Network. The general laboratory configuration is depicted in Figure 4-4. Using this equipment, numerous experiments can be designed to investigate the performance of the AVA/ATV-300 codec as well as the ASX-200BX ATM switches. The SX/14 Data Channel Simulator provides additional flexibility to simulate large end-to-end propagation delays over wired or wireless network environments. The AX4000 Analyzer/Generator is useful for generating background network traffic and presenting network performance data in meaningful formats.

The next chapter will describe the network organization and protocol architecture in greater detail. Experimental procedures and results will also be presented.

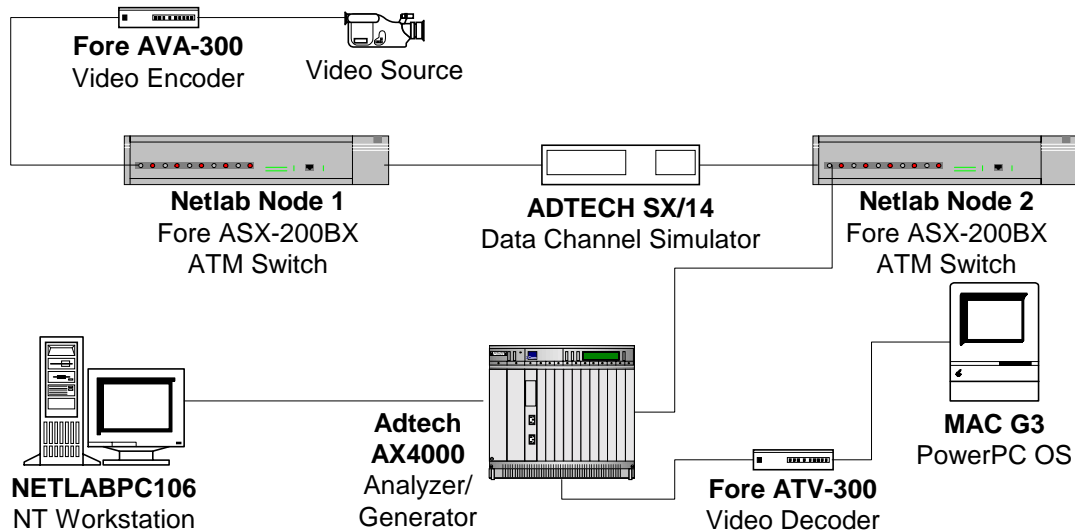


Figure 4-4. Physical Network Configuration.

V. DATA SETS, EXPERIMENTS, AND RESULTS

A. VIDEO DATA SET CHARACTERISTICS

Video clips were chosen based on a qualitative perceptual analysis of their content that included level of action in the video clip, scene complexity, scene-change rate, and image generation technique. The clips ultimately used for experiments reflect significant variations in each of the above qualities. In all cases, the video is rendered as a sequence of frames in 24-bit color with 640×480 resolution. The clips are further categorized into Compression Families as described in Table 5-1. The baseline clips for these experiments are M-JPEG compressed with a Q-Factor of 20 (Compression Family A) and transmitted through a noiseless network environment. A list of the chosen video clips and a short description of their baseline qualities follows. Specific timeline descriptions of each clip are included in Appendix A.

A	30 fps, Q = 20
B	30 fps, Q = 32
C	30 fps, Q = 64
D	30 fps, Q = 128
E	30 fps, Q = 200
F	15 fps, Q = 20
G	15 fps, Q = 200
H	10 fps, Q = 200

Table 5-1. Compression Families.

1. Baseline TARZAN Video Clip

Figure 5-1 displays the time-varying bandwidth requirement in cells per second for the baseline TARZAN video clip. This clip was taken from Disney’s animated feature, “Tarzan” (1999). The clip was chosen as an example of traditionally-produced cartoon animation including scene detail of both high and low complexities. Additionally, the scene-change rate for this clip varies from a “normal” rate at the beginning to a “very high” rate at the end of the clip.² Scene changes are marked by sudden sharp negative peaks in the bandwidth trace.

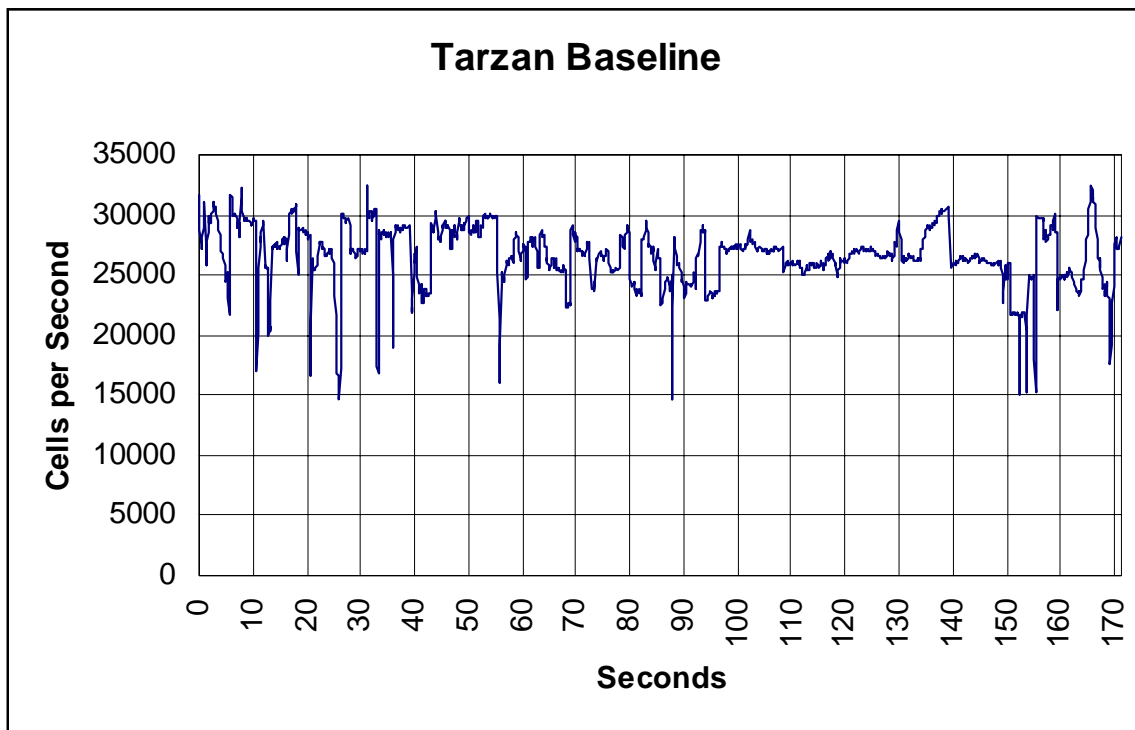


Figure 5-1. TARZAN Baseline Bandwidth Requirement.

² Clips begin on the right hand side of the trace in Figures 5-1 through 5-4. See Appendix A for further information.

2. Baseline TOYSTORY2 Video Clip

Figure 5-2 displays the time-varying bandwidth requirement in cells per second for the baseline TOYSTORY2 video clip. This clip was taken from Disney’s animated feature, “Toy Story 2” (1999). The clip was chosen as an example of computer-generated cartoon animation including moderately complex scene detail. This clip exhibits a “normal” scene-change rate punctuated by short periods of “high” scene-change rates.

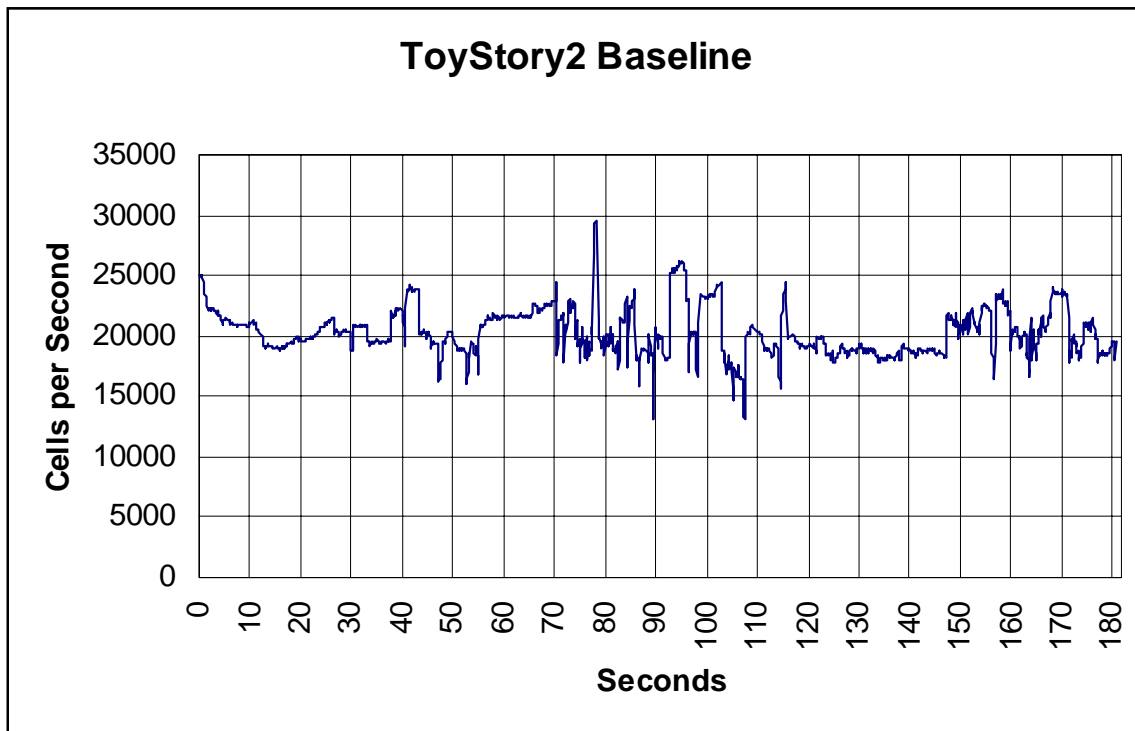


Figure 5-2. TOYSTORY2 Baseline Bandwidth Requirement.

3. Baseline WIZARD Video Clip

Figure 5-3 displays the time-varying bandwidth requirement in cells per second for the baseline WIZARD video clip. This clip was taken from MGM’s musical, “The Wizard of Oz” (1964). The clip was chosen as an example of traditional camera-

generated video of natural subjects including people, forest, and buildings. The clip contains scene detail of high, medium, and low complexity. The scene change rate is considered “low” throughout the clip. This clip is characterized by very crisp and substantial transitions of the bandwidth trace as scenes change from a large scene to a character close-up.

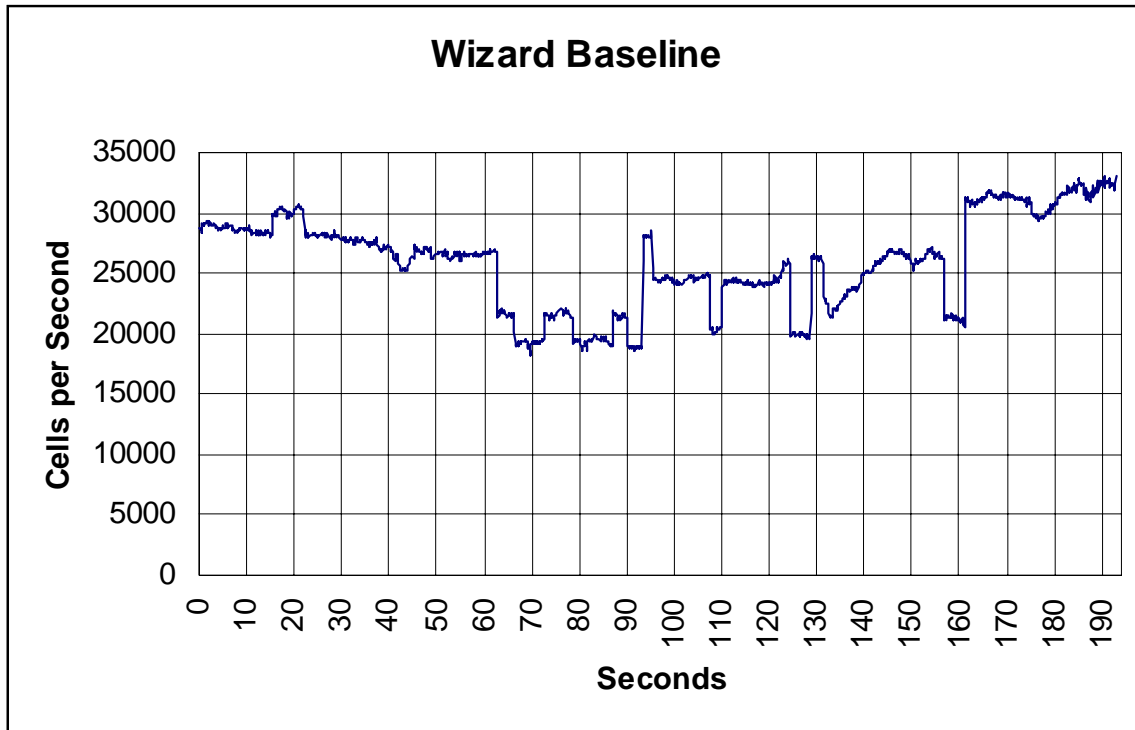


Figure 5-3. WIZARD Baseline Bandwidth Requirement.

4. Baseline DISTANCE Video Clip

Figure 5-4 displays the time-varying bandwidth requirement in cells per second for the baseline DISTANCE video clip. This clip was taken from a live Distance Learning classroom environment at the Naval Postgraduate School. The clip was chosen as an example of a typical business application of networked video technology. The scenes primarily consist of either high-complexity black and white text (first 95 seconds of the clip) or low-complexity black and white text (remainder of the clip). Additionally, the

text contains some occasional simple graphics. There are also several instances where the scene is punctuated by an instructor’s hand, finger, or pointing device. This clip exhibits a “very low” scene-change rate produced only by the occasional zoom or page flip.

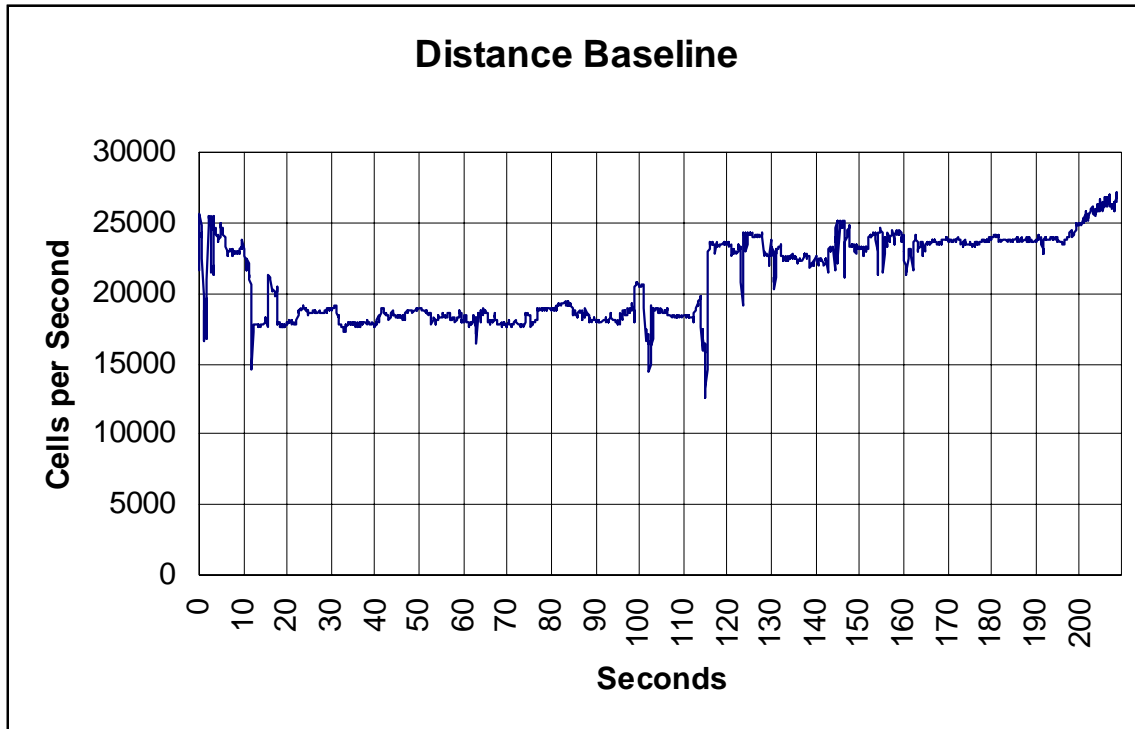


Figure 5-4. DISTANCE Baseline Bandwidth Requirement.

5. Bandwidth Profile Analysis

Due to the effect of M-JPEG compression on the sequence of frames, each of the chosen video clips behaves in a distinctive manner. A bandwidth profile is a histogram representation of a clip’s time-varying bandwidth requirement. The most important portion of the bandwidth profile is the manner in which the histogram tapers off at the high bandwidth limit. Analysis of the histogram will provide insight to the behavior of a particular clip in a managed bandwidth environment such as an ATM network using UPC. Figure 5-5 shows the bandwidth profile for each video clip in Compression Family A.

There are striking differences between the clip profiles. Whereas, the TARZAN and TOYSTORY2 clips conform to approximate Gaussian distributions with one easily identifiable mean, the DISTANCE clip appears approximately Gaussian around two separate concentration values. The WIZARD clip is quite different from the others in that it contains six separate concentration areas with the overall distribution envelope remaining nearly constant.

When planning UPC contracts for these disparate types of video, the bandwidth profile must be taken into consideration. For instance, clips that conform to an approximate Gaussian bandwidth profile might be well suited to a VBR UPC since they have fairly well defined means and only occasionally require a significantly higher bandwidth. Bandwidth allotments for this type of video can be minimized with a predictable affect on perceived quality by setting UPC parameters at a certain point above the main bandwidth profile concentration. Occasional lost cells will have a minimal affect on perceived video quality. On the other hand, clips with more than one area of concentration in their bandwidth profile must use a UPC contract that is based on their highest bandwidth concentration. This leaves little opportunity to take advantage of VBR contracts as a bandwidth management tool as bandwidth allotments for this type of video cannot be minimized very much without significantly impacting the perceived video quality.

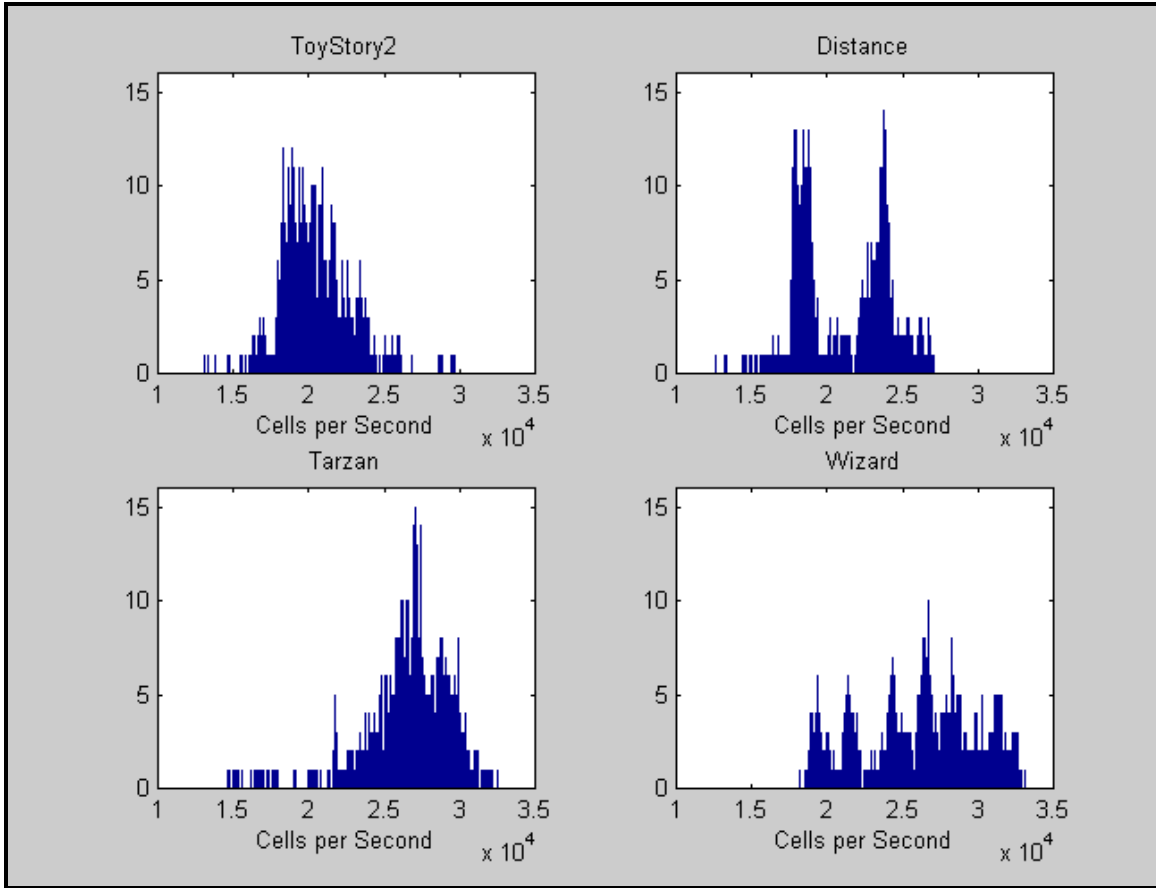


Figure 5-5. Bandwidth Profiles for Baseline Data Sets.

B. ARCHITECTURE, ORGANIZATION, AND PROCEDURES

1. Protocol Architecture

Each experiment in this thesis follows the protocol architecture outlined in Figure 5-6. Original analog video is read from a VCR tape and presented to the M-JPEG encoder in standard NTSC format. The video encoder produces AAL 5 cells at its output for direct input to an ATM network. The SONET physical layer then connects the various network components. Finally, the protocol architecture is reversed and the data is ultimately presented to the user in analog NTSC format.

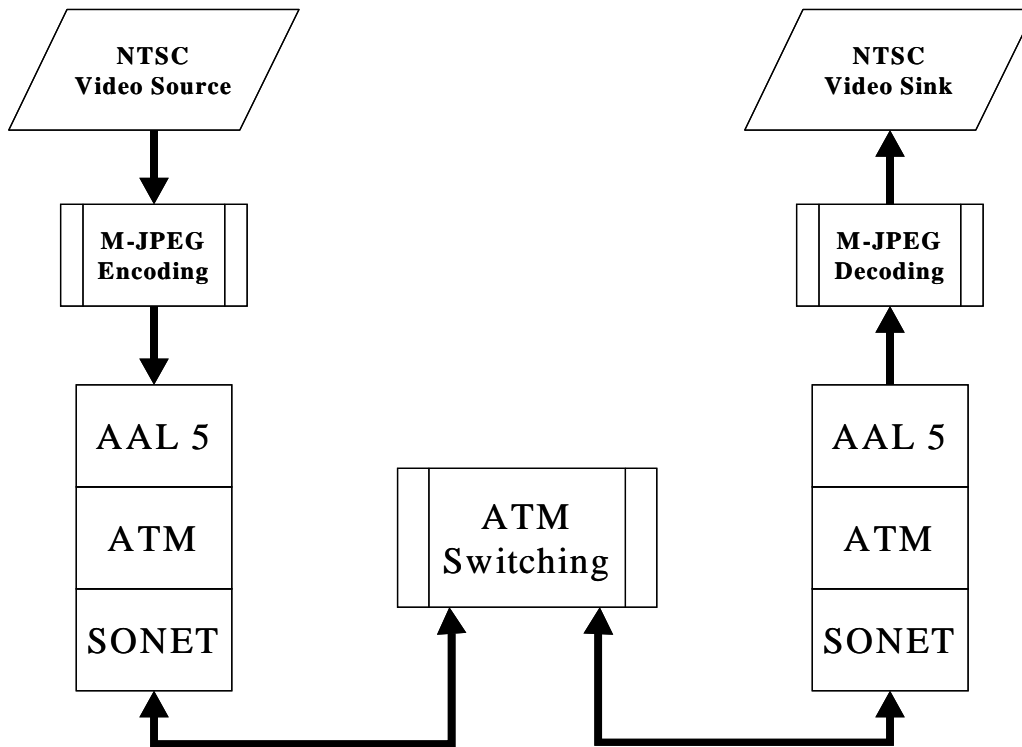


Figure 5-6. Protocol Architecture.

2. Physical Network Description

The Advanced Networking Laboratory's Video Testing Network is depicted in Figure 5-7. Two video sources are available for analog input to the network – a VCR and a Digital Video Camera. These sources provide analog signals directly to the ForeTM AVA-300 Video Encoder. The AVA-300 provides AAL 5 cells directly to the ATM network via an OC-3 link to NETLAB Node 1. The video stream then exits Node 1 on the intermediate range OC-3 port and enters the ADTECHTM SX/14 Data Channel Simulator. The SX/14 simulates delay and error conditions then gives the video stream to NETLAB Node 2 via an OC-3 link to Node 2's intermediate range port.

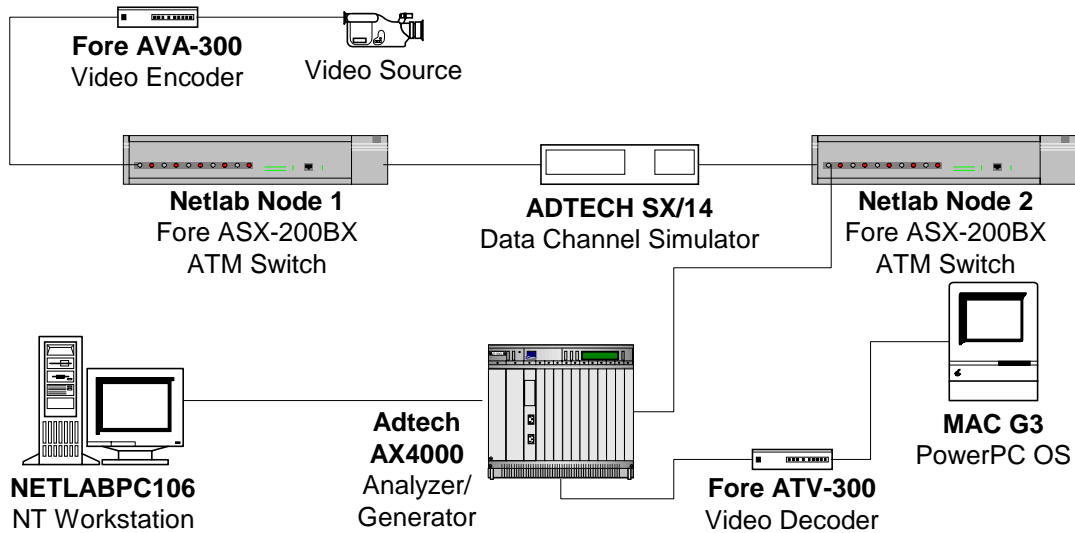


Figure 5-7. Physical Network Configuration.

3. Data Collection Procedures

The first step of each experiment is to enter the planned parameters in the video encoder, ATM switch, and Data Channel Simulator. Then, the software for the AX/4000 is readied to gather data for the experiment. The original video clips are then fed to the AVA-300 for sampling, encoding, and presentation to the ATM layer. The video data is then subject to the admission control and switching algorithms in ASX-200BX Node 1 before noise and/or delay is added in the Data Channel Simulator. ASX-200BX Node 2 then processes the video data and switches it through the AX4000 Analyzer. The resulting performance data is captured by the AX/4000 software while the final video data stream is passed to the ATV-300 for decoding, digital to analog conversion, and presentation. At the conclusion of the experiment, the captured data from the AX4000 is saved as ASCII text for later analysis in MATLAB or Excel.

a. *Effects of Intra-frame Compression on Video Performance*

The set of experiments investigates the effect of intra-frame compression on the instantaneous bandwidth requirements of the given video data sets, their resulting bandwidth profiles, and their cell inter-arrival time characteristics. Instantaneous

bandwidth data for each video clip is obtained for Compression Families A through E and the data is stored for analysis using Microsoft Excel. Additionally, the Compression Family E bandwidth profile is developed for comparison with baseline data sets. Bandwidth profiles for the other compression families are not shown since the incremental changes in the profile characteristics are small and the point of the experiment can easily be made by analyzing just Compression Families A and E.

Since video compression is the focus of this set of this set of experiments, all other network parameters are set to very liberal tolerances to avoid affecting the system in an unplanned manner. Switches are set to allow unrestrained use of bandwidth requiring no adherence to UPC contracts or admission control algorithms. The Data Channel Simulator is set to pass all data without inducing error or unnecessary delay.

b. Effects of Frame Rate on Video Performance

This set of experiments investigates the effect of frame rate on the instantaneous bandwidth requirements of the given video data sets. Instantaneous bandwidth data for each video clip is obtained for Compression Families F and G. This data is stored for analysis using Microsoft Excel.

Since video frame rate is the focus of this set of this set of experiments, all other network parameters are set to very liberal tolerances to avoid affecting the system in an unplanned manner. Switches are set to allow unrestrained use of bandwidth requiring no adherence to UPC contracts or admission control algorithms. The Data Channel Simulator is set to pass all data without inducing error or unnecessary delay.

c. Effects of Bandwidth-Managing UPC Contracts on Video Performance

In the third set of experiments, suitable UPC contract types and parameters are developed for the TOYSTORY2 data set based on the favorable characteristics of its bandwidth profile. In particular, the baseline bandwidth profile for TOYSTORY2 (Figure 5-5) can be approximated by a Gaussian distribution profile. Using this assumption, suitable UPC contracts are designed and programmed into Netlab Node 1 for testing of

video transmission quality under various network constraints. Figure 5-8 illustrates the statistical relationships considered in the design of UPC contracts. Table 5-2 provides details about the various UPC contracts developed for these experiments.

The other bandwidth profiles depicted in Figure 5-5 are not further analyzed because either they display redundant types of characteristics or their characteristics indicate intolerance toward VBR traffic management schemes. For instance, the Tarzan bandwidth profile is very similar to the TOYSTORY2 profile and they produce similar results under the conditions of this experiment. On the other hand, the Distance and Wizard bandwidth profile envelopes do not follow a Gaussian shape. Rather, their characteristics are such that any deviation from a straightforward CBR contract would result in unacceptable loss of video quality. Thus, the analysis of these data sets is not of interest in this set of experiments.

d. Effects of Delay Variation-Managing UPC Contracts on Video Performance

The fourth set of experiments studies highly compressed video (bandwidth below 2.5 Mbps) transmitted through a simulated long-distance ground-to-aircraft video link. For continuity, the TOYSTORY2 video clip is used again in this experiment. The primary purpose of this experiment is to examine the effect of an ATM switch's CDVT on video performance. The high compression factor used in this experiment contributes significant initial CDV to the system, which is exacerbated by various other network parameters. A step-wise delay sequence is programmed into the SX/14 Data Channel Simulator to create the effect of network latency and CDV due to aircraft movement. Appendix B details the delay sequence design. Finally, UPC contracts with very restrictive CDVT parameters are programmed into Netlab Node 2 for the purpose of inducing cell loss. In order to isolate the parameters of the experiment, no noise is inserted into the system and liberal CBR UPCs are employed with CDVT as the only constraining variable.

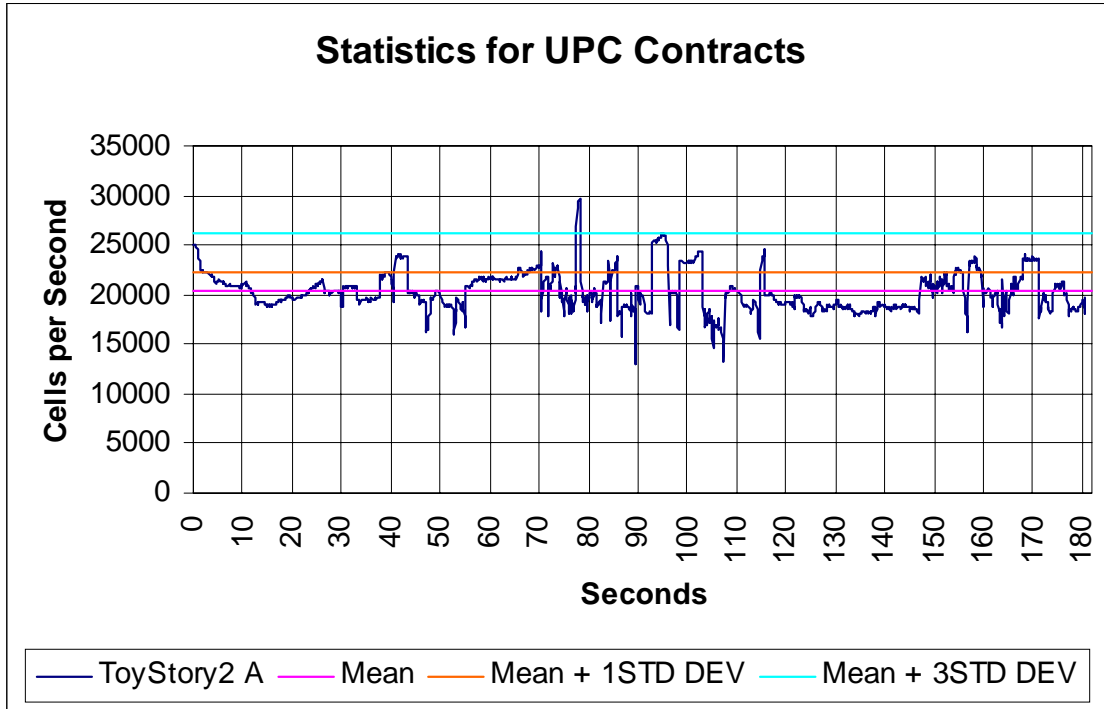


Figure 5-8. Statistics for TOYSTORY2 A.

UPC	TYPE	SCR	PCR	MBS	CDVT
1	CBR	NA	MEAN +1 STD DEV	NA	NA
2	VBR	MEAN +1 STD DEV	MEAN+3 STD DEV	100 msec	NA
3	VBR	MEAN +1 STD DEV	MEAN+3 STD DEV	500 msec	NA
4	VBR	MEAN +1 STD DEV	MEAN+3 STD DEV	750 msec	NA
5	VBR	MEAN +1 STD DEV	MEAN+3 STD DEV	1 sec	NA
6	CBR	NA	20000 CPS	NA	300 μ sec
7	CBR	NA	20000 CPS	NA	225 μ sec

Table 5-2. UPC Contracts.

e. Effects of Noise on Video Performance

Finally, an analysis of M-JPEG video performance in the presence of noise was also attempted. Regrettably, no useful experiments could be developed in this area since the equipment manufacturer denied requests for proprietary information regarding the AVA-300 codec. Some qualitative observations from the preliminary investigations of M-JPEG video performance in a noisy channel follow in Section C of this chapter.

C. RESULTS OF EXPERIMENTS

1. Effect of Intra-frame Compression on Video Data Set Characteristics

Figures 5-9 through 5-12 reflect the instantaneous bandwidth requirements of the subject video clips within each Compression Family. As expected, the primary effect of compression on the video bit stream was to lower the mean bandwidth value. As a secondary effect, the range of bandwidth excursions was narrowed as Q-Factor was increased.

The data in these figures clearly illustrates the expectation that compressing the video stream with the M-JPEG algorithm can minimize bandwidth requirements. In fact, M-JPEG compression has a linear, scaling effect on the instantaneous bandwidth requirement for compression families producing “usable” quality video. Plots of the mean cell rate per compression family, their standard deviations, and percent deviation from the mean are shown in Figure 5-13. Because of this scaling property, further experiments will only create and analyze video data sets (compression families) based on Q-Factors of 20 and 200.

Qualitatively, each increasing level of compression, represented by a higher Q-Factor value, reduces the visual quality of the video. For Compression Family A ($Q = 20$), the resulting visual distortion is entirely unnoticeable. The video appears smooth; texture and edge details are clearly defined. As the experiment progresses through Compression Families B, C, and D, visual quality suffers from the appearance of blocky artifacts, which are characteristic of the JPEG compression algorithm at high compression rates.

Additionally, edges within each video frame display ringing artifacts. This ringing effect is especially detrimental to the quality of the DISTANCE clip. Text presented on the distance learning slides becomes unreadable in the presence of moderate ringing artifacts. Compression Family E produces an extremely low-quality video exhibiting all of the previously mentioned artifacts resulting in a video clip that is very dissatisfying to watch.

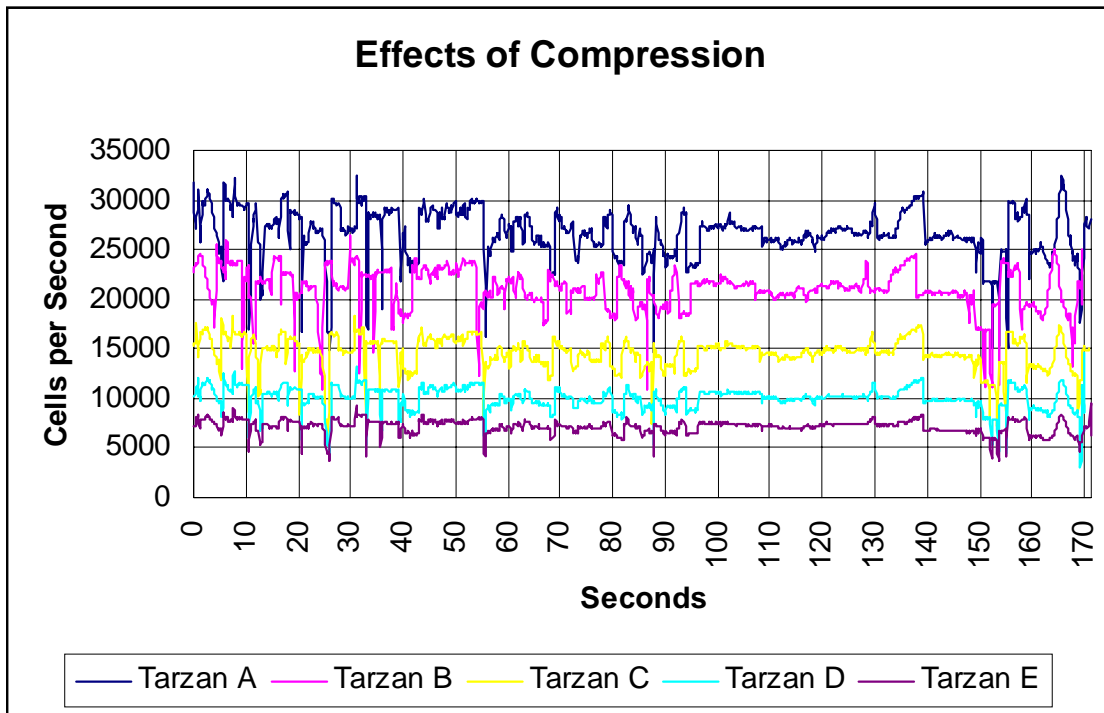


Figure 5-9. Effect of Compression on TARZAN Video Clip.

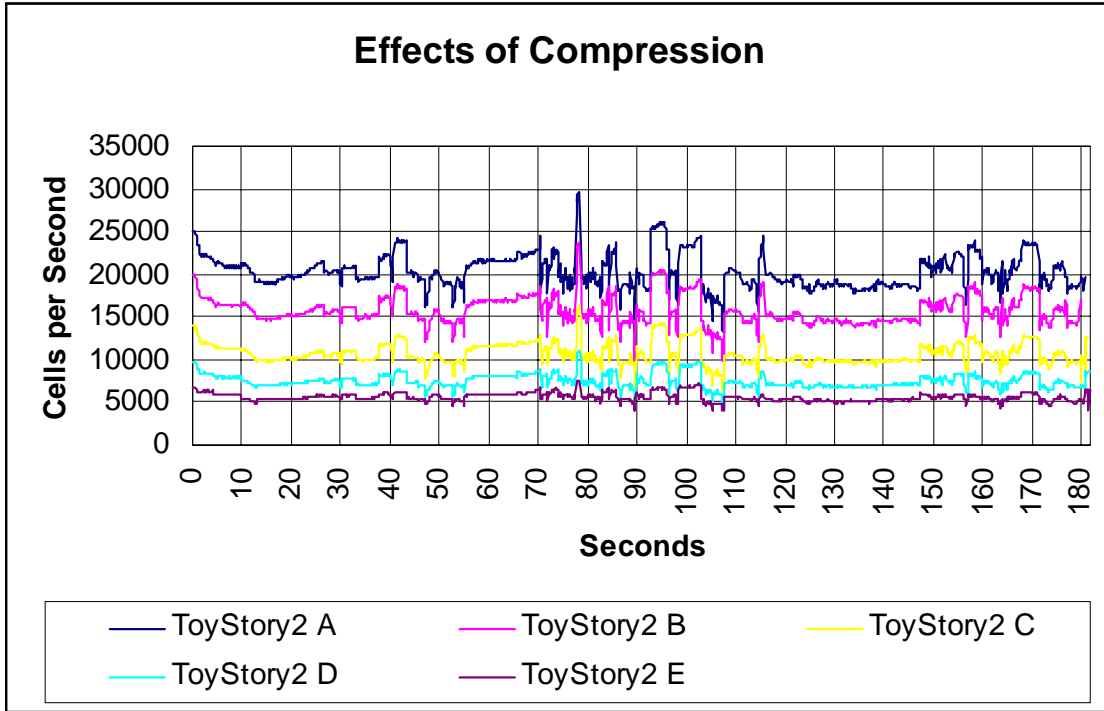


Figure 5-10. Effect of Compression on TOYSTORY2 Video Clip.

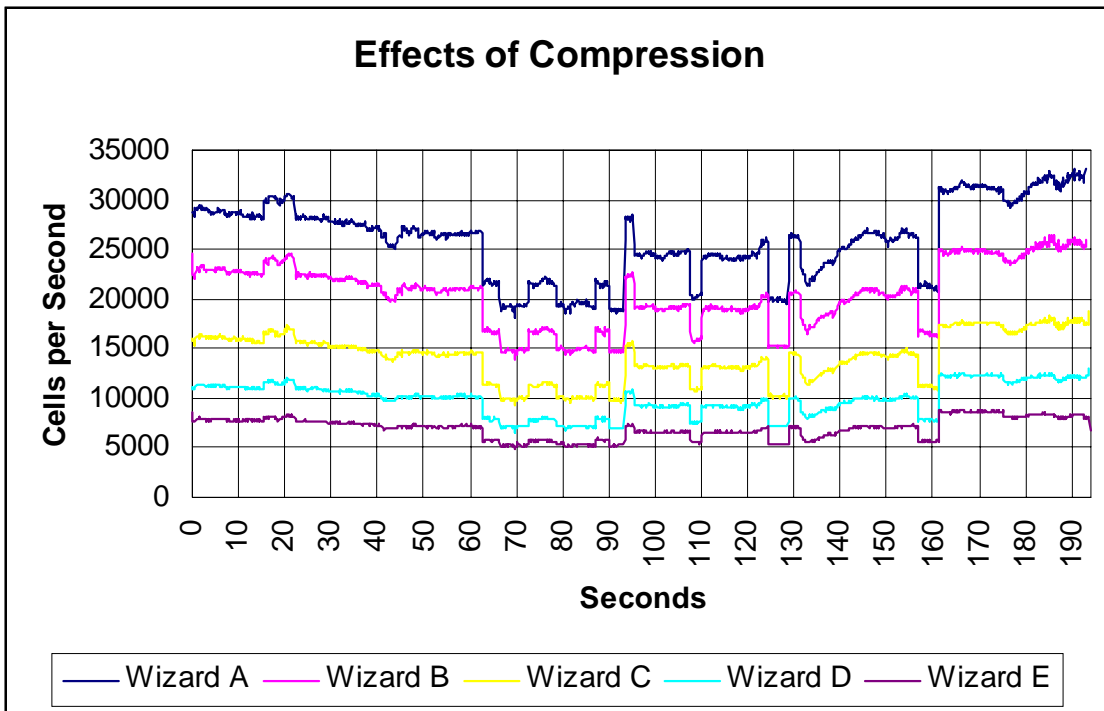


Figure 5-11. Effect Compression on WIZARD Video Clip.

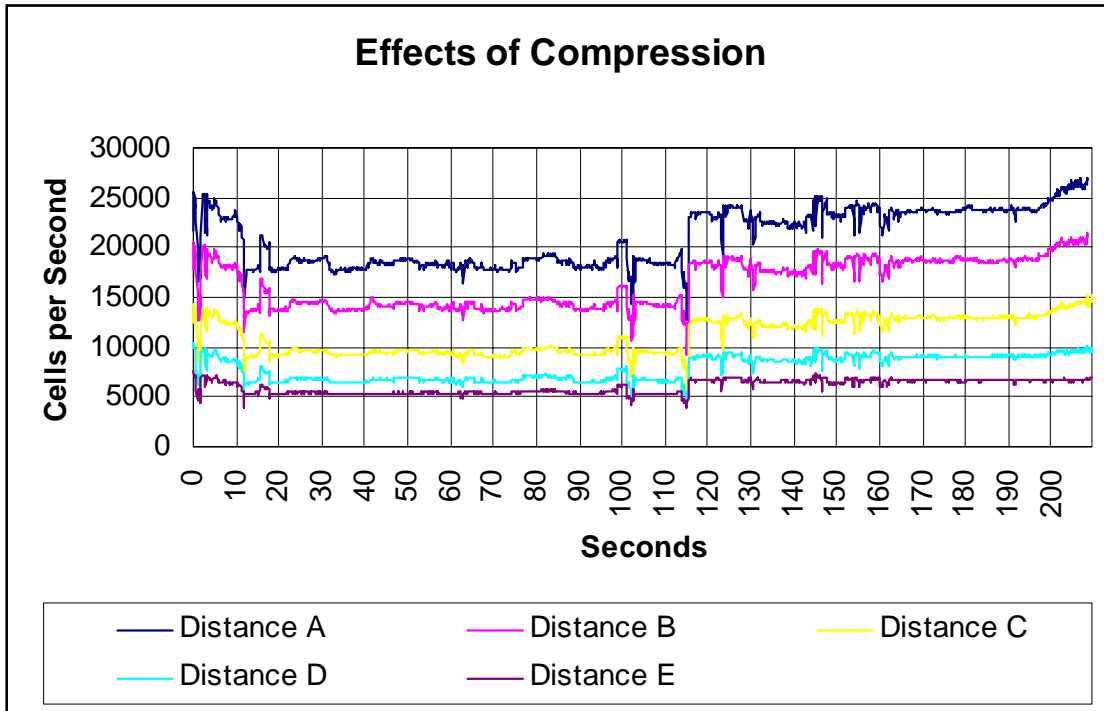
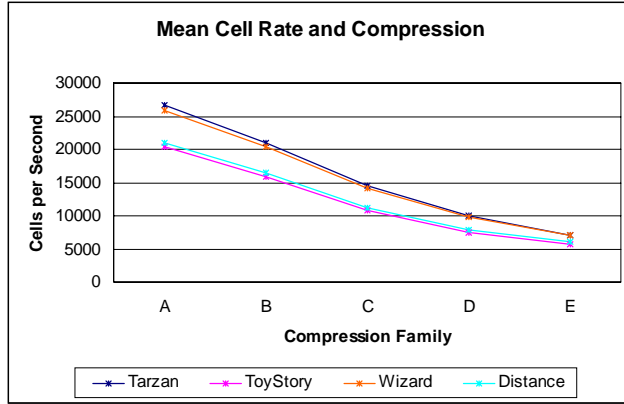
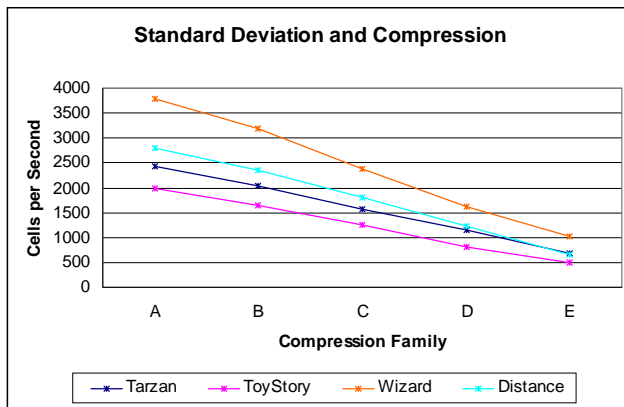


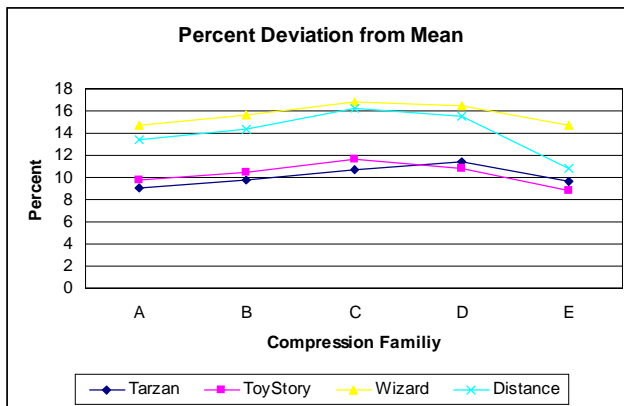
Figure 5-12. Effect of Compression on DISTANCE Video Clip.



(a)



(b)



(c)

Figure 5-13. Linear Effects of Compression on Video Data Sets.

While the linear scaling effect of M-JPEG compression is easily deduced from an understanding of the math behind the process, the effect of M-JPEG compression on the shape of bandwidth profiles presents a more interesting question. Figure 5-14 illustrates that the compression process does not smooth bandwidth profiles. In fact, compression has more clearly defined the multiple concentration areas of the DISTANCE and WIZARD clips. As previously stated, the most suitable UPC contract for these video streams is CBR since the bandwidth profiles have very sharp limits at the high end. Conversely, the TOYSTORY2 and TARZAN clips are good candidates for VBR contracts since their bandwidth profiles taper off gradually at the high end.

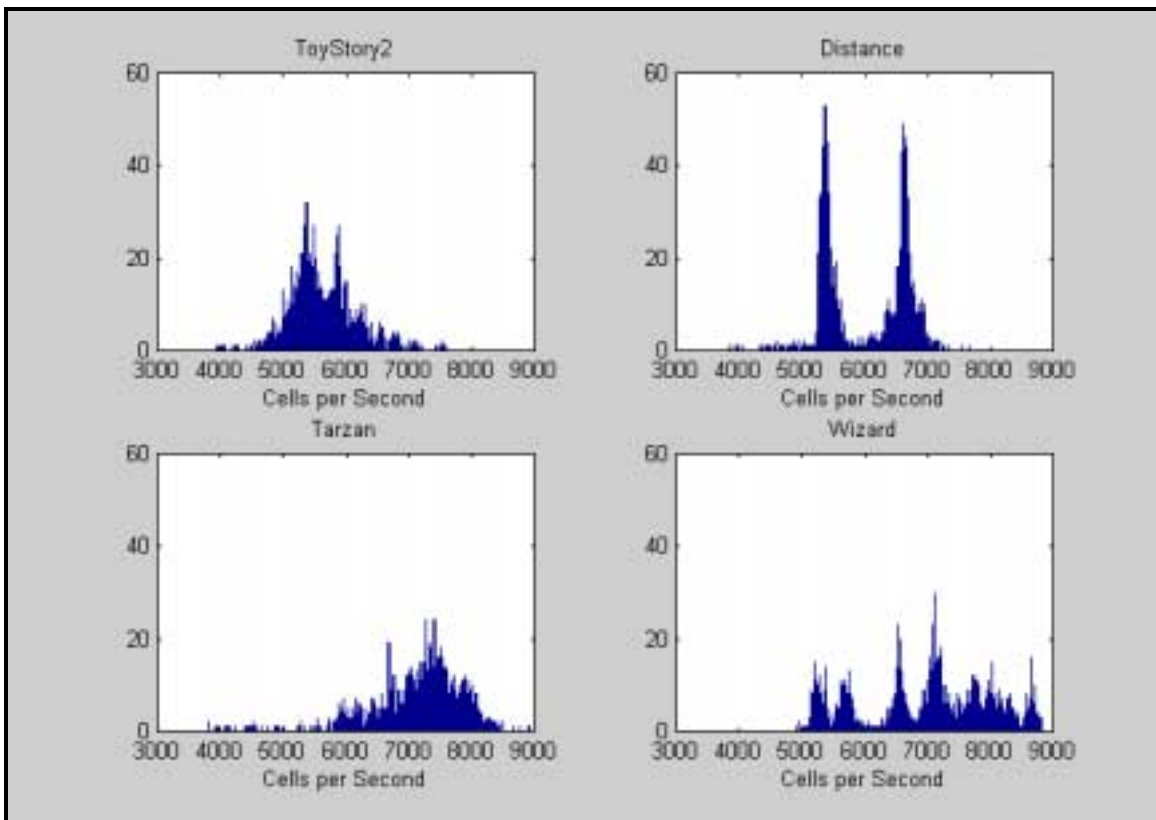


Figure 5-14. Bandwidth Profiles for Compression Family E.

In addition to sharpening the video bandwidth profiles, intra-frame compression also increases the variance in cell inter-arrival times. Normalized histograms of this behavior are plotted in Figures 5-15 through 5-18. Frames containing highly complex

images will not compress very well and, therefore, will fill cell payloads very quickly for a given frame rate. When a set of frames is not very complex, high compression efficiency can be achieved with an accompanying deceleration of the cell arrival rate. This is caused by the fact that an ATM cell will not be released from the video encoder until its payload is full of data. The resulting distribution of cell inter-arrival times can be approximated by an exponential distribution. Note that one special quality of the exponential distribution is that its variance is equal to its mean.

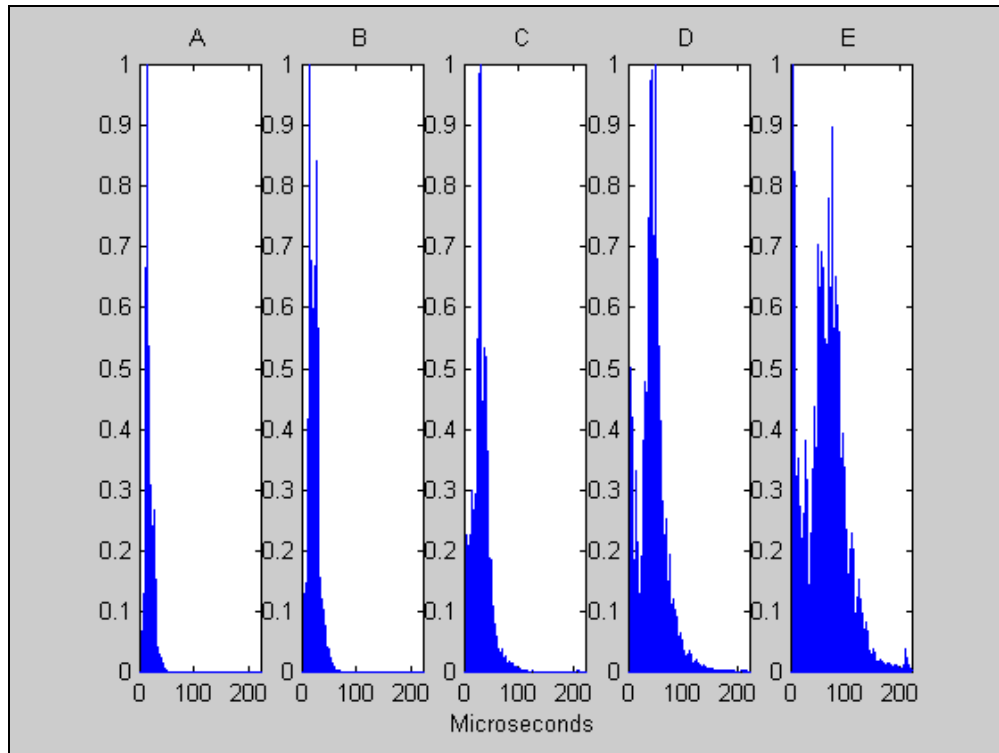


Figure 5-15. Cell Inter-arrival Time for TARZAN Compression Families.

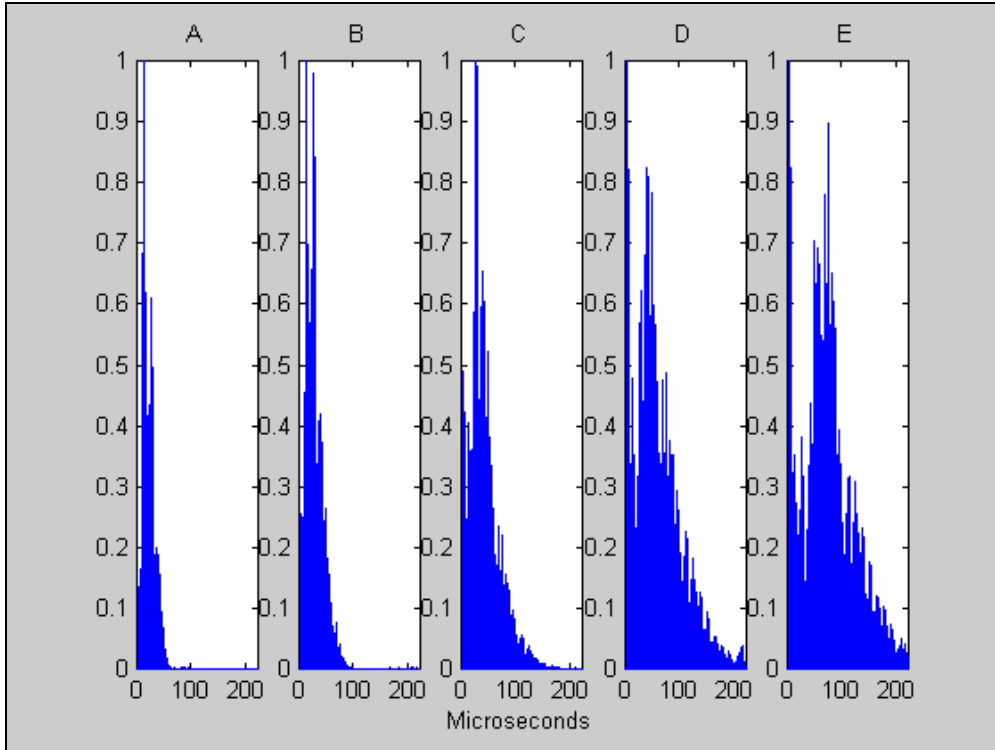


Figure 5-16. Cell Inter-arrival Time for TOYSTORY2 Compression Families.

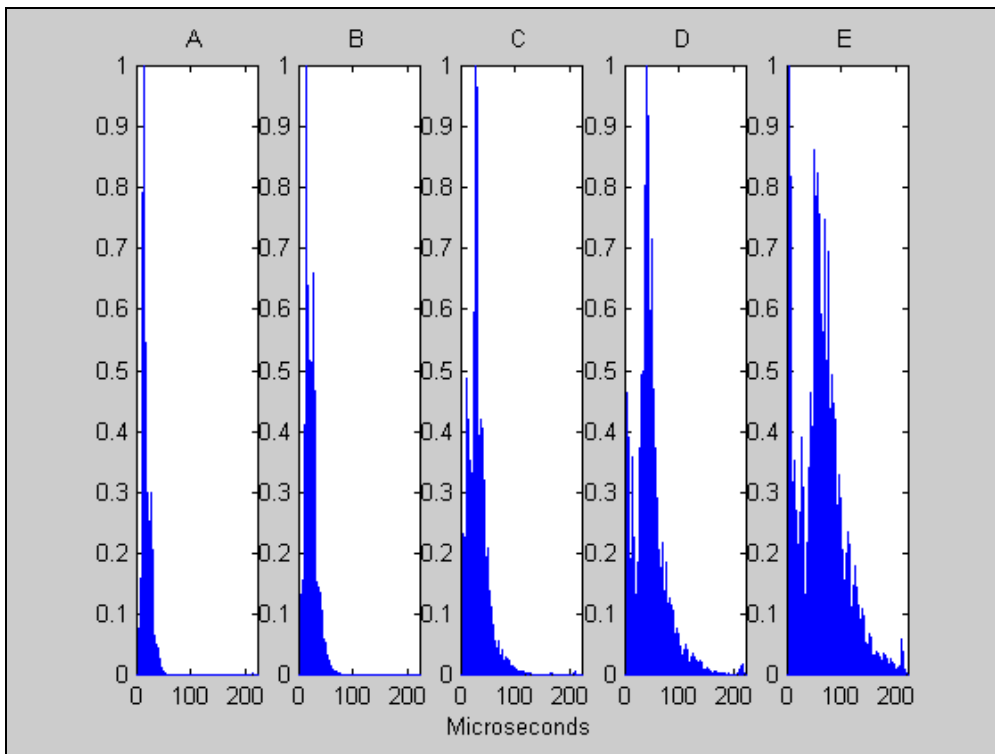


Figure 5-17. Cell Inter-arrival Time for WIZARD Compression Families.

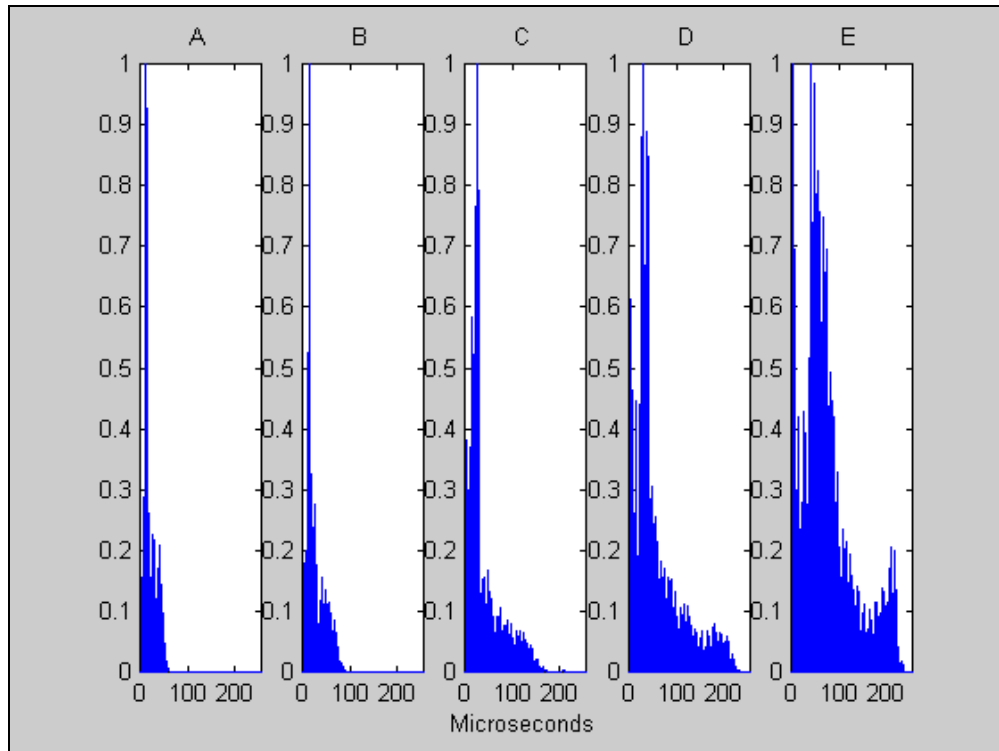


Figure 5-18. Cell Inter-arrival Time for DISTANCE Compression Families.

2. Effect of Frame Rate on Video Data Set Characteristics

Figures 5-19 through 5-22 display the instantaneous bandwidth requirements for Compression Families F and G. As with the previous experiment involving compression, the primary effects of changing the frame rate were lowering of the mean required bandwidth value for each Compression Family and linearly scaling the details of the instantaneous bandwidth requirement trace. In other words, sending half of the original data requires half of the original bandwidth.

Qualitatively, the detrimental effects from frame rate reduction are much more subtle than the effects from increasing compression rate. Visually, start-stop frame staggering is the only artifact introduced by reducing the frame rate of a video. This choppy quality is most noticeable at frame rates below 15 fps and has no effect on the quality of texture and edge details. It is important to note that this choppy quality is very consistent and regular unlike the jitter effects caused by CDV, which will be explored in the fourth experiment.

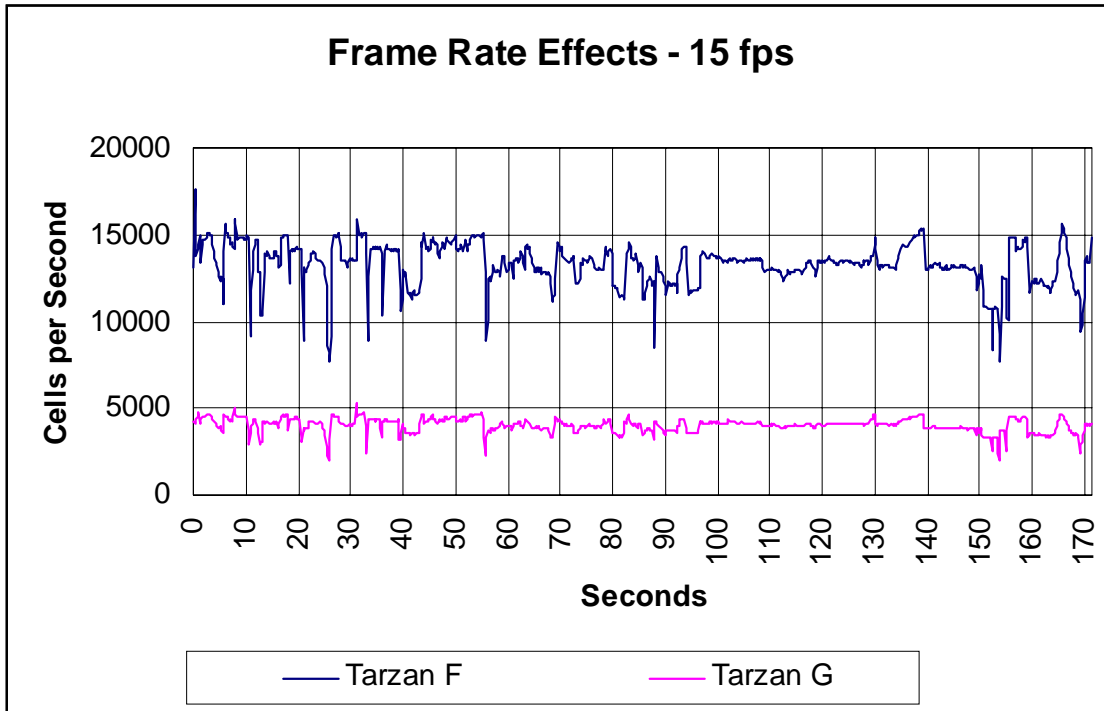


Figure 5-19. Effect of Frame Rate on TARZAN Video Clip.

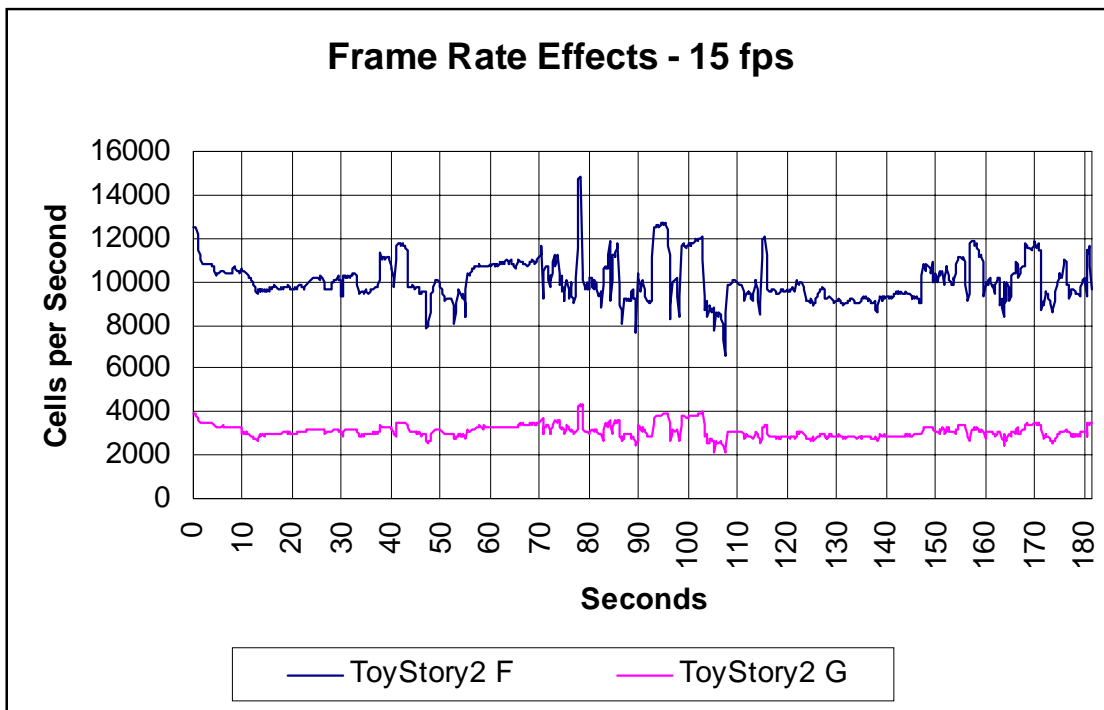


Figure 5-20. Effect of Frame Rate on TOYSTORY2 Video Clip.

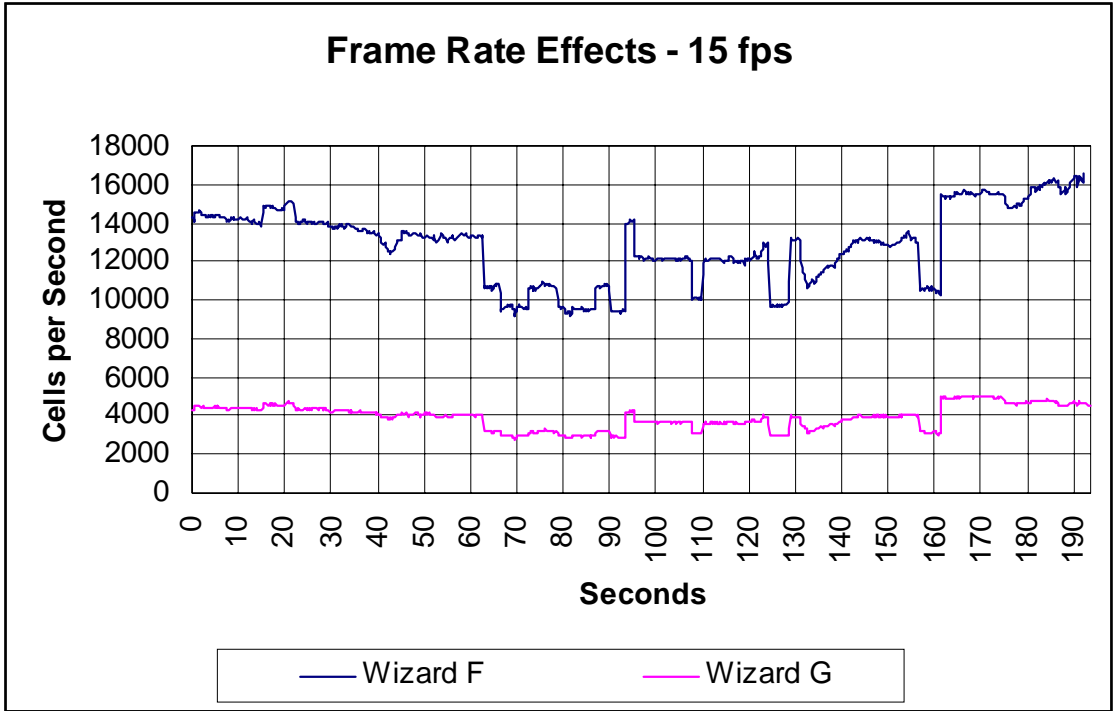


Figure 5-21. Effect of Frame Rate on WIZARD Video Clip.

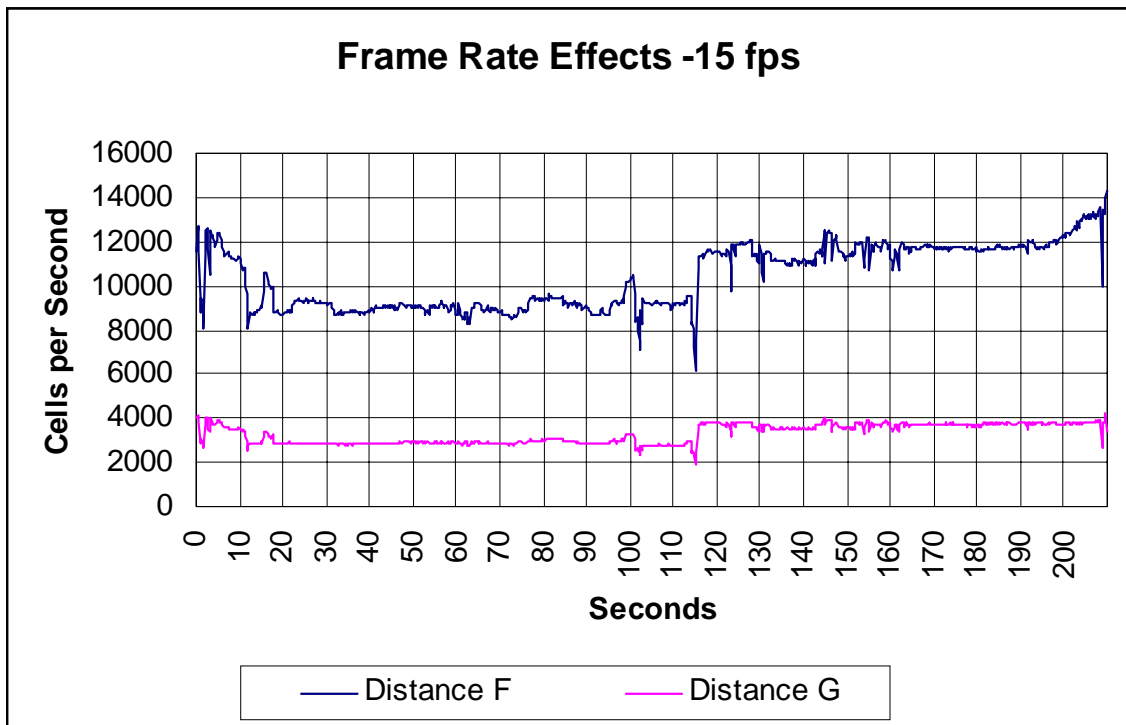


Figure 5-22. Effect of Frame Rate on DISTANCE Video Clip.

3. Effect of UPC on Video Data Set Characteristics

Figures 5-23 through 5-27 portray the effects of various UPC contracts on the instantaneous bandwidth requirements and QoS for Compression Family A of the TOYSTORY2 clip. In each of the figures, the larger top window displays the original instantaneous bandwidth requirement and the resultant instantaneous bandwidth trace after the video stream is passed through a switch employing a selected UPC contract. A bandwidth reference line at one standard deviation above the original mean bandwidth requirement is shown in Figure 5-23. For readability, this line is not shown in the remaining figures. The bottom two windows in each figure focus in on selected areas of the instantaneous bandwidth trace for more detailed analysis of the dropped cell behavior and recovery.

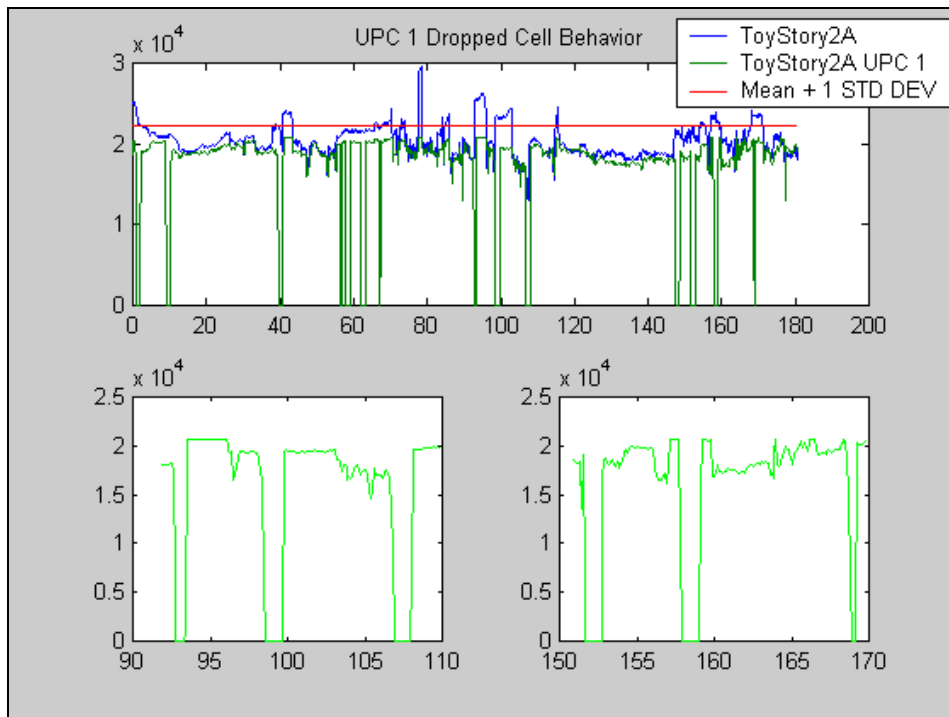


Figure 5-23. Effect of UPC 1 on TOYSTORY2.

Figure 5-23 depicts the video behavior of the TOYSTORY2 clip under a CBR UPC constraint. In this case, the upper limit of the CBR contract is set at the a priori mean bandwidth requirement plus one standard deviation. The original Compression

Family A version of the TOYSTORY2 bandwidth trace is plotted for reference along with the same trace under the UPC 1 constraint.

Analysis of Figure 5-23 shows that the UPC 1 contract causes excessive cell loss whenever the instantaneous bandwidth requirement exceeds the CBR parameter. Additionally, the traces between indices 55-70 and 145-155 indicate that the bandwidth allocation does not immediately return to its assigned parameter upon relief from the contract violation condition. In each of these cases, the instantaneous bandwidth requirement is at or just below the UPC 1 CBR parameter. In effect, the policing mechanism within the ASX-200BX switch attempts to limit cell throughput to a level below the maximum allowable bit rate whenever the instantaneous bandwidth approaches the stipulated CBR limit.

A similar analysis is shown in Figure 5-24 using a VBR UPC where $SCR = \text{Mean} + 1 \text{ STD DEV}$ and $PCR = \text{Mean} + 3 \text{ STD DEV}$. (Bandwidth reference lines are excluded for clarity.) This UPC drops fewer cells than UPC 1 and maintains a closer match with the original TOYSTORY2A bandwidth trace. Another interesting observation can be made with respect to the error recovery behavior for this UPC. The UPC 2 contract allows the system to recover faster than the UPC 1 contract as evidenced by the catastrophic cell loss events between indices 90 and 100 (see Figures 5-24 and 5-25).

Other VBR UPCs are similarly analyzed in Figures 5-25 through 5-27 with the only change of parameter being an increase in MBS. For UPC 3, Figure 5-25 shows an increase in catastrophic cell loss events over the UPC 2 example while the system recovery behavior appears similar to that of UPC 2. For UPCs 4 and 5 the number of catastrophic cell loss events is decreased but in each case, however, system recovery is slower than the UPC 3 case.

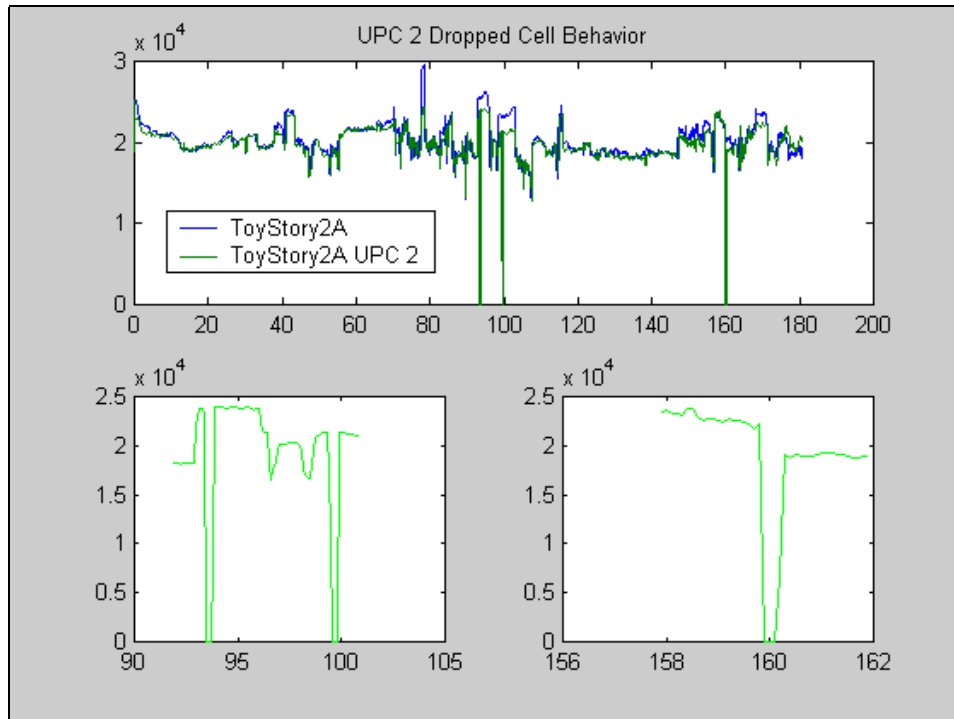


Figure 5-24. Effect of UPC 2 on TOYSTORY2.

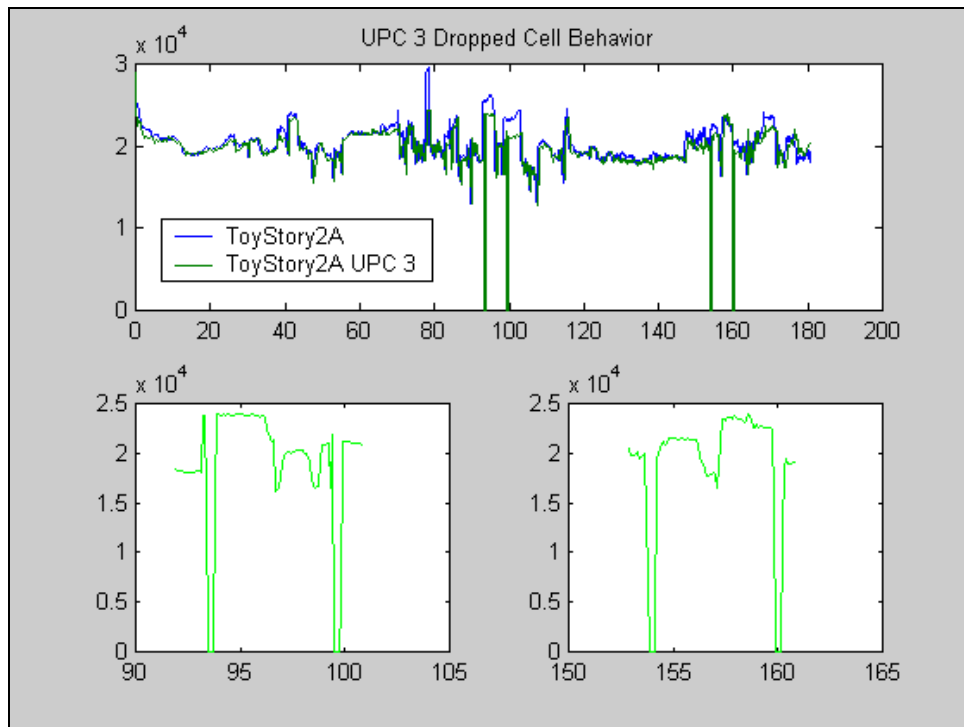


Figure 5-25. Effect of UPC 3 on TOYSTORY2.

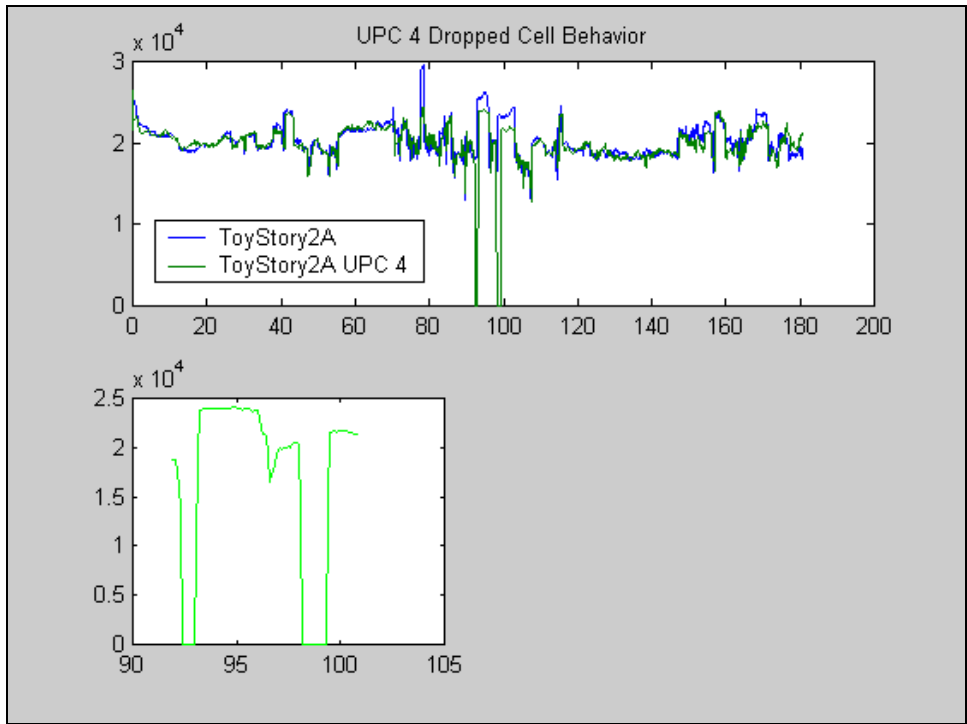


Figure 5-26. Effect of UPC 4 on TOYSTORY2.

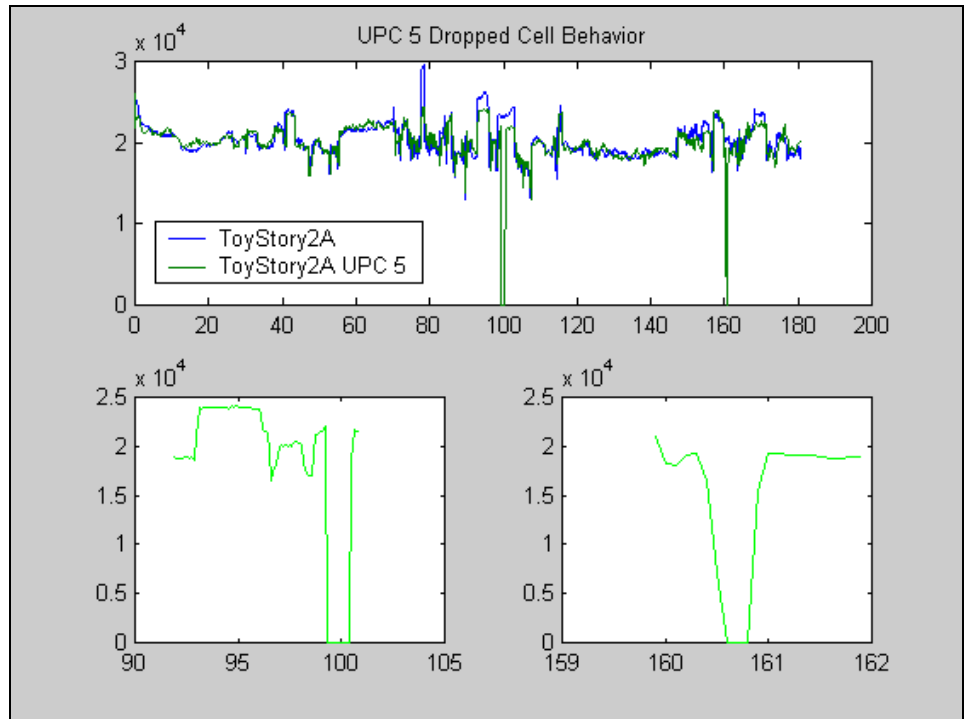


Figure 5-27. Effect of UPC 5 on TOYSTORY2.

In qualitative terms, visual effects of the UPC contracts employed in this set of experiments were very harsh. This was expected since the experiment is designed to operate on the upper edge of the TOYSTORY2 bandwidth profile. Accordingly, a moderate rate of cell discard is experienced throughout the video clip with isolated catastrophic cell loss events occurring for severe violations of the designated UPC contract.

Moderate cell discard rates are visually characterized by a certain number of contiguous blocks missing from a M-JPEG frame. These blocks tend to be contiguous since one ATM cell will contain several consecutive blocks from the original M-JPEG frame. When a cell is discarded, the error is visually manifested as a rectangular disturbance within the frame. The ATV-300 decoder utilizes error concealment to compensate for the lost blocks of data during periods of moderate cell loss (See Figures 5-23 to 5-27: the bandwidth trace between indices 150 through 170 provides a good example of this behavior). The visual effect of this error concealment technique is essentially a “pausing” of the block data from the previous frame. In most cases, this older data fits nicely into the current frame due to the high degree of inter-frame correlation. However, if the error occurs across less correlated frames such as a scene change or period of significant motion, use of the concealment technique is very noticeable.

Catastrophic cell loss events result in total loss of video with an accompanying loss of ATV-300 decoder synchronization. This situation is visually characterized as a sequence of solid blue frames, the default no-signal output from the ATV-300 decoder. This behavior is recorded as max-low excursions of the instantaneous bandwidth traces in Figures 5-23 through 5-27. It is interesting to note that, when catastrophic cell loss events occur in this clip, they happen in two specific timeframes. Specifically, they happen when higher than average bandwidth requirements extended for a long period of time. During each of these periods, the original video clip is very complex in terms of its motion and scene complexity. These intricate frames lead to compression inefficiency in the AVA-300, which results in a higher bandwidth requirement to maintain a constant frame rate.

As the ATM switch processes this over-budget bandwidth requirement, the GCRA will discard cells according to the established UPC.

4. Effect of Cell Delay Variation on M-JPEG Video Performance

Figures 5-28 and 5-29 depict the results of CDVT-based UPCs on Compression Family H of the TOYSTORY2 clip. Trials of only two UPCs are included in the results because the window of interesting results for this type of contract turned out to be very narrow. When CDVT was set above 300 μ Sec, the visual and measured effects of the restriction were unremarkable. When CDVT was set below 225 μ Sec, no usable video passed through the network. The AX/4000 would register sporadic bursts of cells but the visual output from the entire video system remained nil.

One area of difficulty encountered in performing this experiment involved undesirable artifacts introduced by the SX/14 Data Channel Simulator. While the SX/14 can easily change its bit error modes and parameters on a programmed basis, it has difficulty making a smooth transition between programmed delay or data rate modes and parameters. A new delay buffer must be calculated and set whenever these parameters are changed, which causes a noticeable discontinuity in the data stream.

The purpose of the SX/14 in this set of experiments was to generate CDV. Therefore, the delay parameter was changed at the minimum programmable step interval of one second. This procedure introduced periodic artifacts that can be seen in the instantaneous bandwidth traces of Figures 5-28 and 5-29. There is no visual evidence that cells are lost in the buffer recalculation operation. However, this procedure introduces unmeasured delay and variation into the experiment and detracts from the realism of any simulation.

Overall, the CDVT-based UPCs used in this set of experiments did not significantly affect the output bandwidth trace. Aside from the previously mentioned SX/14 artifacts and a minimal rate of cell discard due to CDV, there was very little deviation from the original bandwidth trace. These low cell discard rates were visually characterized by the same block error disturbance discussed previously. Interestingly, the

visual effect of block error concealment actually improved the quality of the video by countering the CDV jitter effect during periods of minimal cell discard. However, when a more restrictive CDVT parameter was set, cell discard rates increased. The ATV-300 then used error concealment to compensate for the lost data thereby creating a staggered frame visual effect. This effect was similar to the results seen previously in the second set of experiments (i.e. lowering the frame rate of the video encoder).

This behavior was again caused by decreased compression efficiency as the AVA-300 processed a sequence of intricate video frames. To maintain a constant frame rate, each of these intricate frames requires transmission at an above average cell rate. As a result, the CDV changes abruptly and exceeds the parameters of the designated UPC contract. The ATM switch then discarded cells to alleviate the UPC violation, which eventually triggered catastrophic cell loss.

Catastrophic cell loss behavior consistently occurred at one of the same high-bandwidth peaks that triggered cell loss in the previous experiment (see Figures 5-28 and 5-29 at approximate index 100). As the system encountered catastrophic cell loss in this set of experiments, the cell loss events were not characterized by the default no-signal output from the ATV-300 decoder. Rather, the error concealment mechanism within the decoder was able to respond to the problem without loss of internal synchronization. In this case, the concealment technique had the visual effect of “pausing” entire frames until the UPC violation was alleviated.

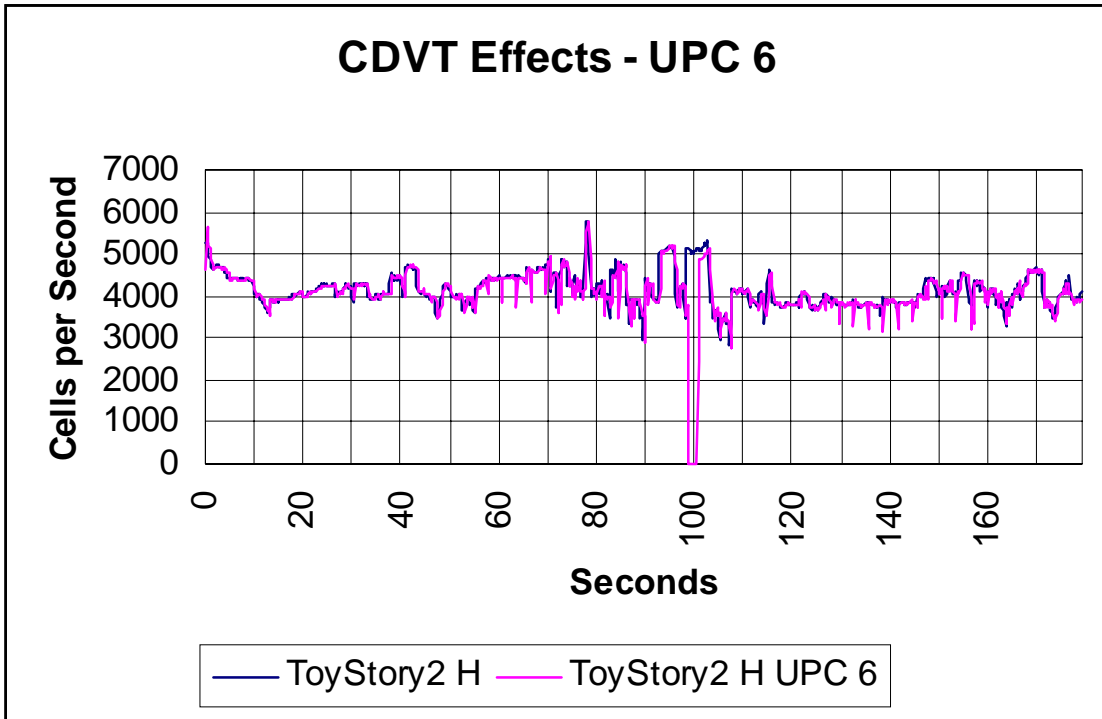


Figure 5-28. Effect of CDVT on TOYSTORY2 Video Clip (CDVT = 300 μ Sec).

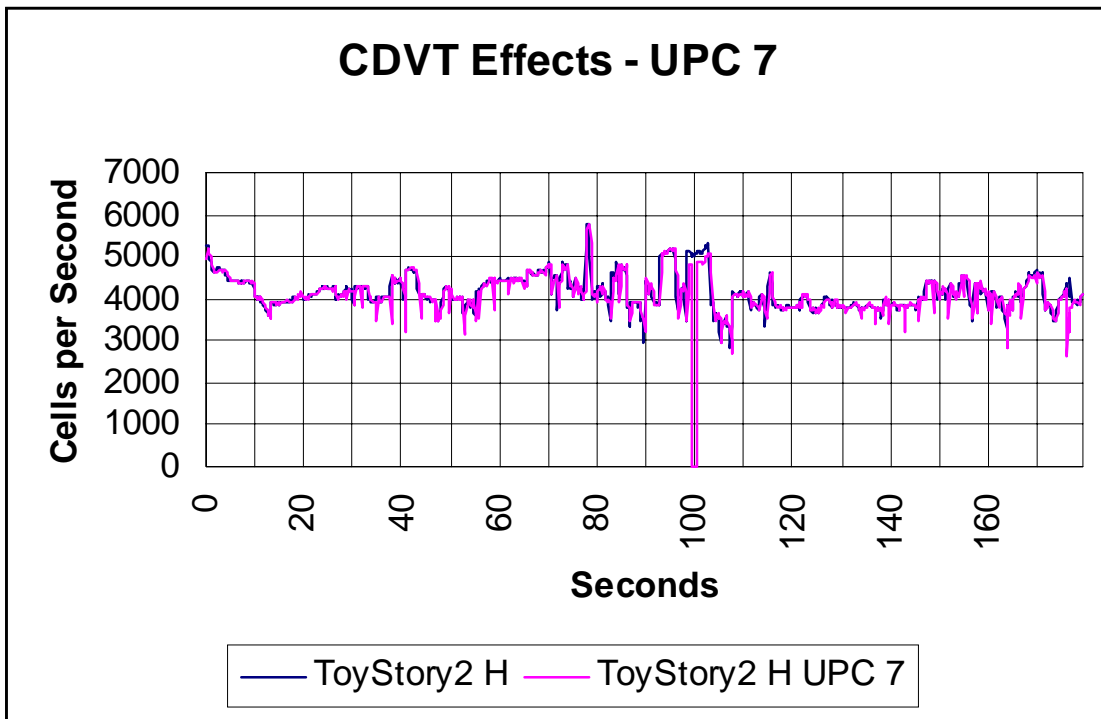


Figure 5-29. Effect of CDVT on TOYSTORY2 Video Clip (CDVT = 225 μ Sec).

5. Effect of Noise on M-JPEG Video Performance

Starting with a simulated white noise environment, video clips were run through the network of Figure 5-7. In general, the encoded video stream was very robust to white noise interference, which is not surprising since the AVA-300 codec is a commercial off-the-shelf product. The expected “fuzzy” picture generally caused by the presence of white noise did not appear for any arbitrary noise parameter values. However, for all noise parameters, the video did suffer occurrences of packet loss and/or synchronization problems, which seemed to get more severe with the addition of more white noise. In essence, video quality was limited by the fragility of the network protocol architecture; the primary encoded data stream was actually very robust to noise effects.

Packet loss errors were characterized by the visual effect of small, horizontal rectangular sections of data missing from the displayed video frame. The AVA-300 codec performed error concealment for this situation by filling the missing rectangle with data from a previous good frame, but the effect was still quite noticeable since there is no inter-frame prediction mechanism in the M-JPEG standard.

Synchronization problems caused by the presence of white noise can be split into two varieties, intra-frame decoder synchronization effects and multi-frame network synchronization effects. Intra-frame decoder synchronization errors are characterized by the total loss of current-frame data after a certain point in the video frame. Suffering an error in one or more critical JPEG header bytes probably causes this. The resulting video frame contains some number of properly decoded blocks from the intended image followed by a default visual error pattern that fills the remaining portion of the frame. More intense noise conditions lead to loss of network synchronization, which results in the loss of multi-frame video data. Under this condition, the AVA-300 simply replaces several consecutive video frames with the default no-signal blue screen until network synchronization is reestablished.

D. SUMMARY

The first portion of this chapter characterized the baseline data sets chosen for system analysis. The design, purpose, and procedural details for each experiment were then discussed. Finally, quantitative and qualitative analyses of the experimental results concluded the chapter.

Experiments performed in this chapter include quantitative and qualitative investigation of the effects of intra-frame compression, reduction of video frame rate, ATM bandwidth and cell delay management algorithms, and transmission channel noise on M-JPEG video performance. After examining the baseline characteristics of the video data sets in the first set of experiments, the TOYSTORY2 video was chosen as the most appropriate clip for further experimentation. This clip was processed and transmitted over the experimental ATM network under various constraints according to the design of each particular experiment. Quantitative and qualitative analysis of the network's performance is then presented for each experimental condition.

During the course of these experiments, several limitations of the laboratory design and equipment were discovered. For instance, the SX/14 Data Channel Simulator introduced artifacts to the experiments under certain conditions. Additionally, any analysis of image processing and channel coding procedures within the AVA/ATV-300 codec is limited by minimal access to system parameters and a lack of technical documentation available from the manufacturer. With more granular access to AVA/ATV-300 system parameters and a more detailed set of system documentation, several interesting experiments could be designed to assess the robustness of the M-JPEG implementation to channel noise.

The next chapter will discuss the overall conclusions of this thesis and recommendations for further work.

THIS PAGE INTENTIONALLY LEFT BLANK

VI. CONCLUSIONS AND RECOMMENDATIONS

The objective of this thesis was to analyze the performance of a commercially available intra-frame coded video application under various constraints within an ATM network. Concurrently, a packet video experimentation module was developed within the Advanced Networking Laboratory.

A. CONCLUSIONS REGARDING BANDWIDTH MANAGEMENT

When conforming to austere bandwidth limitations, one can achieve similar bandwidth efficiencies by employing either image compression techniques or simple frame rate reduction. (In general, other bandwidth-reduction options exist, such as adjusting the spatial resolution and quantization granularity of the encoder. However, these parameters are not accessible with the equipment used in this thesis.) The cost, in terms of perceived quality, is different for each option. Use of an image compression technique, such as M-JPEG, produces blockiness and ringing artifacts in the video output for increasing levels of compression. Alternatively, reducing the frame rate of the video will produce a staggering effect in the video output. Since perceived quality is very subjective, an optimal combination of these techniques will depend on the particular type of video and the audience.

Owing to the bandwidth profile characteristics generated in certain types of video applications, tightly bounded VBR UPCs may perform no better than straight-forward CBR contracts. Specifically, when a bandwidth profile contains several narrow bandwidth concentrations, only the concentration nearest the upper limit can be manipulated without causing severe degradation in perceived quality. This type of bandwidth profile is generated by video containing panoramic and/or zoom clips, such as movies and distance learning applications. Conversely, both traditional and digitally-created animation clips produced approximately Gaussian bandwidth profiles. This type of video was somewhat more amenable to VBR UPC contracts.

Whenever UPC contracts were employed in this thesis, the limits of the contract were designed with very tight parameters that were customized to the data. As expected, each of these contracts produced cell loss errors with some scenarios extending to complete loss of network synchronization. In each instance, the network recovered from catastrophic failure when the instantaneous bandwidth or CDV parameters were no longer in violation of the UPC contract. Notably, differences appeared in the recovery time characteristics for various UPC settings. However, it is unclear how much of this recovery behavior is due to continuing cell loss for extended UPC violations and how much is due to network and decoder resynchronization latency.

B. CONCLUSIONS REGARDING SECOND ORDER DELAY

Cell delay by itself is not a critical performance factor in an ATM network unless the network provides service to time-sensitive media applications, such as interactive voice or video. However, the second order delay statistic, CDV, plays a crucial role in multimedia QoS regardless of whether the applications are interactive or not. When there is significant CDV, a visual (or audio) effect known as “jitter” is produced in the media output stream. Excessive jitter can be very disruptive to a media application because it produces uneven staggering of media frames resulting in a very low perception of quality from the customer point of view.

In this thesis, CDV was naturally generated due to the computational complexity of the M-JPEG compression scheme. Intricate frames requiring more computational resources and bandwidth left the encoder at a slower rate than the simple frames. Additional CDV was induced through programming a sequence of step delays into the SX/14 Data Channel Simulator. Once again, these UPC parameters caused cell loss during high complexity portions of the video clip. In general, the visual effects of jitter were exacerbated by a tightly regulated CDVT. In addition to the jitter effect, discarding cells that violated the CDVT caused a visual staggering effect in the output similar to decreasing the frame rate.

C. CONCLUSIONS REGARDING PERFORMANCE IN NOISE

Even though the technical details of the AVA/ATV-300 codec were not available, it is apparent that the codec is quite robust to channel noise. As mentioned previously, the video did not suffer the expected “fuzzy” degradation when subjected to white noise. Rather, the codec was able to correct or compensate for the noise. The ATM network proved to be the weakest link under noisy channel conditions. When noise levels started affecting critical bytes of the SONET and ATM protocol structures, the network lost synchronization resulting in complete loss of video output until network synchronization could be reestablished.

D. RECOMMENDATIONS FOR FUTURE WORK

There are numerous opportunities for future research using the system described in this thesis. While the focus of this thesis has been packet video, the packet audio capabilities of this system have yet to be explored. Whether considering audio or video, experiments can be developed to focus on the DSP components, the networking components, or the communications channel. Parameters for each of these components are accessible to the user in varying degrees of detail.

Whenever compressed data is transmitted through a noisy channel, there is a trade-off between compression efficiency and the fragility of the compression protocol. In other words, some bits in the data stream take on more significance than others in the decoding process. In the compressed domain, a single well-placed error can render a large number of bits useless. With this in mind, a study could be developed to target particular bits in M-JPEG, ATM, or SONET protocol structures. It would be interesting to identify critical bits in each of these protocols and, perhaps, design mechanisms to protect them under noisy channel conditions.

Similarly, if the internal design details of the AVA/ATV-300 codec were made available, several interesting communications theory experiments could be developed. For example, an analysis of the robustness and efficiency of the source and channel

encoding schemes could be conducted. On the DSP side, the decoder's error concealment mechanism could be examined in detail.

Finally, it is important to determine the system's performance when several video streams are competing for the same network resources. This experiment could be conducted by simulating video source traffic from the AX/4000, by running additional video sources through the AVA-300 encoder, or by using a combination of both.

APPENDIX A: VIDEO TIMELINES

When analyzing the baseline bandwidth requirements in Figures 5-1 through 5-4 with reference to the actual video clips used in this thesis, one's orientation in reading the Figures must be from *right to left*. As this data was collected by the AX/4000 software, the newest data points were added to the *left* of the older data points. This arrangement of data does not affect most numerical analyses of the data, however, it makes a significant difference when performing a subjective comparison between the data sets and the actual video. The following timelines describe the selected video clips and provide time indices to the primary events taking place in each clip.

A. TARZAN VIDEO CLIP

170	Camera pans through foliage toward ground
165	Apes appear
155	Close-up of teapot
145	Elephant hiding
140	Close-up of ape & magnifying glass
125	Typewriter scene
110	Ape rips paper, smashes dish
95	Picture obscured by smoke
55	Elephant balancing/dancing on globe
45	Flag pole, Several fast scene changes
10	Apes float in bubbles
1	End of clip

B. TOYSTORY2 VIDEO CLIP

- 180 Bo-Peep and other characters near large white door
- 175 Door bursts open & dog runs in
- 170 Dog runs around child's room and scatters toys
- 135 Door opens, child enters
- 100 Pig addressing a large formation of little green army men
- 70 Mother appears in scene
- 55 Woody is put up on shelf
- 10 Group picture (toy characters)
- 1 End of clip

C. WIZARD VIDEO CLIP

- 190 Camera pans down through foliage
- 180 Dorothy's house appears
- 170 See Dorothy walking
- 160 Zoom in to Dorothy and Toto
- 155 Zoom out, watch bubble fly in from distance
- 131 Good Witch appears from bubble
- 129 Zoom in
- 125 Zoom out to include Dorothy and Good Witch
- 110 Toto close up
- 107 Zoom out to include Dorothy and Good Witch
- 95 Scene change to Wicked Witch feet trapped under house

- 94 Zoom Dorothy
- 90 Zoom Good Witch
- 87 Zoom Dorothy
- 63 Zoom out both Dorothy and Good Witch
- 45 First appearance of Munchkins
- 23 Many Munchkins parade by
- 15 Pan out from village
- 1 End of clip

D. DISTANCE VIDEO CLIP

- 210 Hand waves across scene
- 200 Finger points around
- 165 Page moved up
- 160 Hand in picture
- 145 Zoom in
- 135 Finger pointing
- 128 Page move up
- 117 Page change – less complex now
- 102 Page change
- 100 Zoom out
- 85 Pointing
- 50 Hand in picture
- 40 Hand out of picture

- 30 Hand in picture
- 17 Page change
- 12 Page change
- 10 Finger pointing
- 5 Page change
- 1 End of clip

APPENDIX B: DATA CHANNEL SIMULATOR PROGRAMMING FOR CDV

This particular video application is based on the concept of maintaining a video link between a military shore facility and an airborne Command and Control or Reconnaissance aircraft. Obviously, the aircraft must be simulated in motion at a realistic airspeed. Once the airspeed is chosen and converted to miles per hour, the induced CDV can be calculated. For this experiment, the effects of air temperature, altitude, and wind velocity are ignored and airspeed is assumed to be equivalent to groundspeed.

The airspeed chosen for this simulation was 194 knots, or 223 miles per hour. This airspeed is maintained on a track heading directly away from the shore-based network transceiver. The aircraft holds this course for 21 seconds and then instantaneously turns around and heads back along the same course for 21 seconds. This simulated flight path is repeated continuously for the duration of the experiment. Admittedly, there are some practical inconsistencies with this simulation. Certainly, a loitering aircraft would maintain course for much longer than 21 seconds and the actual turn rate of the aircraft would change the induced CDV during the turn. However, programming a fully realistic flight path into the SX/14 proved excessively tedious with no apparent benefit to the outcome of the experiment. Acknowledging that this pattern of loitering is unrealistic from an aeronautical point of view, the simulation serves its purpose of maintaining a controlled CDV for the duration of the experiment.

The CDV simulation is adjusted for a baseline delay of 1000 μ sec, which equates to a distance of 150 kilometers from the shore base to the aircraft. Every third step of the SX/14 program, the delay parameter is incremented by 1 μ sec. (Recall that the minimum step interval for the SX-14 is one second.) After 21 program steps, the sequence is repeated backwards simulating the return leg of the aircraft's flight path. This program provides a step-wise linear change in delay which translates to an induced variance of 4.35366 seconds.

THIS PAGE INTENTIONALLY LEFT BLANK

LIST OF REFERENCES

1. Cisco Systems, Inc., "LightStream 2020 System Overview: ATM Technology." [<http://www.cisco.com/univercd/cc/td/doc/product/atm/l2020/2020r21x/sysover/atmtech.htm>]. 1997.
2. Fore Systems, Inc. *StreamRunnerTM AVA/ATV User's Manual* MANU0188-04 – March 1999.
3. ATM Forum, Traffic Management Specification, n. AF-TM-0121.000, *Traffic Management Specification Version 4.1*, March 1999.
4. ATM Forum, *UNI 3.0 User Network Interface Specification*, Englewood Cliffs, New Jersey, Prentice-Hall, Inc., 1993.
5. Fore Systems, Inc. *ForeRunnerTM ATM Switch Network Configuration Manual* MANU0148-03 – December 1997.
6. Black, U., *ATM: Foundation for Broadband Networks*, Englewood Cliffs, New Jersey, Prentice-Hall, Inc., 1995.
7. G. K. Wallace, "The JPEG Still Picture Compression Standard", *Communications of the ACM*, Volume 34, No 4, pp. 30-44, April 1991.
8. G. A. Coffey, "Video over ATM Networks." [http://www.cis.ohio-state.edu/~jain/cis788-97/video_over_atm/index.htm]. August 1997.
9. Acharya, S., Smith, B., "Compressed Domain Transcoding of MPEG", *Proceedings of the IEEE International Conference on Multimedia Computing and Systems*, June 28 – July 1, 1998, Austin, TX.
10. Sayood, K., *Introduction to Data Compression*, San Francisco, California, Morgan Kaufmann, 2000.
11. I. G. Richardson, M. J. Riley, "Digital Video Coding" [<http://umi.eee.rgu.ac.uk/umi/digvid/dvhome.html>]. March 1997.
12. Fore Systems, Inc. *ForeRunnerTM ATM Switch User's Manual* MANU0149-01 – March 1997.
13. Adtech, Inc., *SX/14 Data Channel Simulator Operating Manual Version 2.0e*, 1995.
14. Adtech, Inc., *AX/4000 Broadband Test System Manual Version 1.0*, M494-A, 1999.
15. Luoma, M., Kilkki, K., Karjalainen, H., Rahko, K., "Experiences with ATM Equipment and Network Operation", *Trettende Nordiske Teletrafikkseminaret (NTS-13)*, Trondheim, 20-22 August 1996.

16. Kaul, M., Breiteneder, C., Gibbs, S., Heiden, W., Steinberg, D., Wasserschaff, M., "Distributed Video Production over ATM", *Proceedings of the European Conference on Multimedia Applications, Services and Techniques (ECMAST'96)*, Bordeaux, France, 20-24 May 1996.

INITIAL DISTRIBUTION LIST

1. Defense Technical Information Center2
8725 John J. Kingman Road, Ste 0944
Fort Belvoir, VA 22060-6218
2. Dudley Knox Library2
Naval Postgraduate School
411 Dyer Road
Monterey, California 93943-5101
3. Chairman, Code EC1
Department of Electrical and Computer Engineering
Naval Postgraduate School
Monterey, California 93943-5121
4. Professor John C. McEachen, Code EC/Mj.....2
Department of Electrical and Computer Engineering
Naval Postgraduate School
Monterey, California 93943-5121
5. Professor Murali Tummala, Code EC/Tu1
Department of Electrical and Computer Engineering
Naval Postgraduate School
Monterey, California 93943-5121
6. LCDR Albert C. Kinney, USN2
1301 West Main St.
West Plains, MO 65775